Comparative X-ray Structure Analyses of Multidentate Transition Metal Complexes

A thesis submitted in partial fulfilment of the
requirements for the Degree
of
Master of Science in Chemistry
at the
University of Canterbury
by

Kelly-Jayne Flood

July 2006

Table of Contents

Acknowledgments

First and foremost I would like to thank my supervisors, Dr Jan Wikaira and Professor Ward Robinson, for their support and encouragement. I would like to thank Ward for spending hours sitting with me at the computers in the early days, explaining the ins and outs of X-ray crystallography. I would especially like to thank Jan for being available constantly even though her schedule was always, to say the very least, hectic. I need to mention that I was Jan's first student and I really hope that the experience hasn't put you off Jan!

Thanks to Professor Vickie McKee and Professor Neil Curtis for all your help and allowing me to work on your ligands.

Thanks to the Hartshorn and Steel groups for allowing me to "live" with them for some of the duration of my project. In particular I would like to thank; Ramin for his help in the lab, Matt for answering all my questions anytime, William for his help with crystallography, and Jeni for the surfing, shopping and food. Thanks to Associate Professor Richard Hartshorn and Professor Peter Steel for making me feel like part of the 'team' by allowing me to join all the group activities.

Special thanks to Steve Aitkin for all his synthetic help and removing the bung from the $SOCl_2$ many times! Thanks to Bruce Clark for his help with my mass spectra and Rewi Thompson for NMR assistance.

I would like to thank my parents for supporting and feeding me throughout my time at university. I know that you thought it would never-end. But now it has so I promise that one day I will do the same for you, or at least pay someone to do it.

Last but not least, I have to thank my partner, Simon. I don't think that anyone else would have been so patient with me in all my stressed-out glory! It must be the teacher in you. Thank you for all your help, encouragement and telling me to "just get on with it" when I needed to hear it.

Abstract

The biological significance of macrocyclic complexes has been recognized since they were first synthesized by Neil Curtis. They have the potential to play a critical role in mimicking metalloprotein active sites. Nine Curtis macrocyclic complexes have been studied using X-ray crystallographic techniques. Their structures have been solved and comparisons of the results have been made.

Biological importance is also true of the macrocyclic counterpart; side-off and end-off compartmental ligands. In some circumstances these types of ligands are more appropriate because they have extra flexibility due to their pendant arms not being fixed in place by another head-unit, like a traditional macrocycle.

The synthesis of a proposed compartmental ligand; 2,2-(N,N'-bis(benzimidazole-2-ylmethyl)methylamine-5,5'-di-*tert*-butyl-3,3'methanediyl-dibenzyl alcohol (Ligand 1(L1)), has been proposed and outlined. The pendant arms: bis(benzimidazole-2-ylmethyl)amine (BBIM), were successfully synthesized and characterized with ^{1}H NMR, IR and X-ray crystallography. The head-unit: 5,5'-Di-*tert*-butyl-2,2'-dihydroxy-3,3'-methanediyl-dibenzene methanol (DHTMBA), of L1 was synthesized and characterized using ^{1}H NMR, IR and mass spectrometry. A similar head-unit; 5,5'-Di-methyl-2,2'-dihydroxy-3,3'-methanediyl-dibenzene methanol (DHMMBA), was synthesized in an effort to shorten the synthetic time of the head-unit. This was consequently converted to the chlorine analogue; 3,3'-Bis(chloromethyl)-5,5'-dimethyl-2,2'-methane-diyldiphenol (Cl-DHMMB), and characterized with ^{1}H NMR, IR and X-ray crystallography.

Efforts were made to synthesize Ligand 1, but due to synthetic difficulties and time restraints this proved unsuccessful. Suggestions have been made to develop this synthesis.

Abbreviations

BBIM	Bis(benzimidazole-2-ylmethyl)amine
BTBP	2,6-Bis(hydroxymethyl)-4-*tert*-butylphenol
Cl-DHMMB	3,3'-Bis(chloromethyl)-5,5'-dimethyl-2,2'-methanediyldiphenol
Cl-DHTMB	3,3'-Bis(chloromethyl)-5,5'-di-*tert*-butyl-2,2'-methanediyldiphenol
Co13Cl	(3,3-dimethyl-1,5,8,11-tetraazacyclotridecane) dichlorocobalt(III) perchlorate
COCO	*trans*-(12,12-dimethyl-1,4,7,10-tetraazacyclo-tetradecane)diisothiocyanaocobalt(III) tetraisocyanatozinc(II) ethanol solvate
DCM	Dichloromethane
DFMP	2,6-Diformyl methylphenol.
DHMMBA	5,5'-Di-methyl-2,2'-dihydroxy-3,3'-methanediyl-dibenzene methanol
DHTMBA	5,5'-Di-*tert*-butyl-2,2'-dihydroxy-3,3'-methanediyl-dibenzene methanol
HL-Im	2,6-Bis[(bis((1-methylimidazol-2-y1)methyl) amino)-methyl]-4-methylphenol
IR	infra-red
L1	Ligand 1; 2,2-(N,N'-bis(benzimidazole-2-ylmethyl)methyl amine-5,5'-ditertiobutyl-3,3'methanediyl-dibenzyl alcohol
NCA	(5,7,7,13-tetramethyl-13-nitro-1,4,8,11-tetraaza-cyclo-tetradec-4-ene)-nickel(II) tetrachlorozincate
NCC	(2,4,4,10,10,12-octamethyl-1,5,9,13-tetraazacyclo-hexadeca-1,11-diene)-isothiocyanatocopper(II) perchlorate

NCD	N-rac-(5,5,7,12,14,14-hexamethyl-1,4,8,11-tetraaza-cyclotetradeca-7,11-diene)copper(II) perchlorate
NiCu	Di-μ-cyano-1:2κ2 C:N;1:3κ2 C:N-dicyano-1κ2 C-bis-(N-rac-5,7,7,12,12,14-hexamethyl-1,4,8,11-tetraazacyclo-tetra deca-4,1 (14)-diene)copper(II)-nickel(II) tetra cyano-κ1 C) nickelate(II)
NiMeKF	6SR,7RS-(4,6-diethyl-6-methyl-3,7-diazanon-3-ene-1,9-diamine)nickel(II) tetrachlorozincate
NiMeKFR	5SR,7RS-(4,5-dimethyl-3,7-diazanon-3-ene-1,9-diamine)nickel(II) tetrachlorozincate
NiMePh	(5,12-dimethyl-7,13-diphenyl-1,4,8,11-tetraaza-cyclotetradecane) diisothiocyanatonickel(II) acetone solvate
NMR	Nuclear Magnetic Resonance
ppm	parts per million
PSII.	Photosystem II.
THF	Tetrahydrofuran

Chapter 1

1 Introduction

1.1 Introduction

There are two parts to this thesis; crystallographic studies and synthetic work. The crystallographic work was based on compounds provided by Professor Curtis from Victoria University in Wellington. Each compound was investigated using X-ray crystallography to give the structures of these compounds. The structures were compared and the differences have been highlighted in Chapter Two.

The synthetic work was based on a compartmental ligand; 2,2-(N,N'-bis-(benzimidazole-2-ylmethyl)methyl amine-5,5'-ditertiobutyl-3,3'methanediyl-dibenzyl alcohol, (Ligand 1 (L1)) (figure 1.1). The synthesis of which is discussed in detail in Chapter Three. This introduction details the history of the macrocycles.

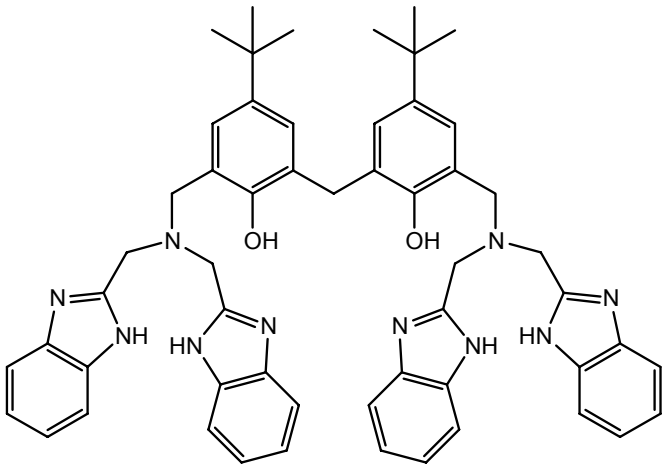

Figure 1.1: 2,2-(N,N'-bis(benzimidazole-2-ylmethyl)methyl amine-5,5'-ditertiobutyl-3,3'methanediyl-dibenzyl alcohol (L1)

1.2 Macrocycles

1.2.1 Curtis Macrocycles

In 1961 Curtis and House proposed the structure of the first macrocyclic ligand (figure 1.2).[1] This was the introduction of azamacrocycles. Since then Curtis has led the field of mononucleating azamacrocycles. A Curtis macrocycle is an organic framework which holds a transition metal ion via nitrogen atoms, with varying substituents on the carbon atoms. These Curtis macrocycles are formed from the reaction of transition metal diamine complexes with acetone in a 2 + 2 condensation reaction.[2] Two acetone molecules are used to form the head-unit. These are condensed with metal ethylenediamine complexes, an example of this is $[Ni(en)_3][(ClO_4)_2]$ which forms the side arms, to complete a cyclic Schiff-base structure.[2]

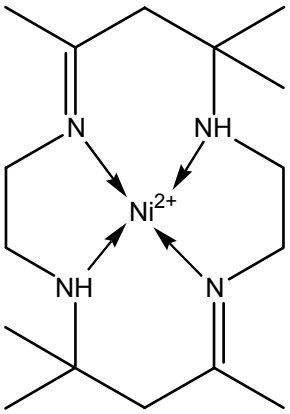

Figure 1.2: Structure of the first macrocyclic ligand; 5,7,7,12,14,14-hexamethyl-1,4,8,11-tetraazacyclotetradeca-4,11-diene

Macrocycles became of interest because of the effects they incur on the metals to which they are coordinated. This is due to the fact that macrocycles have fixed geometries because they form a framework to which the metal is coordinated. Therefore the macrocycle is able to impose its geometry on the metal, which can lead to altered properties of the metal. However, in most cases cooperation to give geometries between those preferred by the metal and the macrocycle are encountered.[3]

1.2.2 Robson Macrocycles

In 1970 Robson[4] produced the first dinucleating Schiff-base macrocyclic ligand (figure 1.3) using 1,3-diaminopropane and 2,6-diformyl-4-methylphenol (DFMP). Since then phenol based ligands have played a large role in macrocyclic chemistry.[5-9]

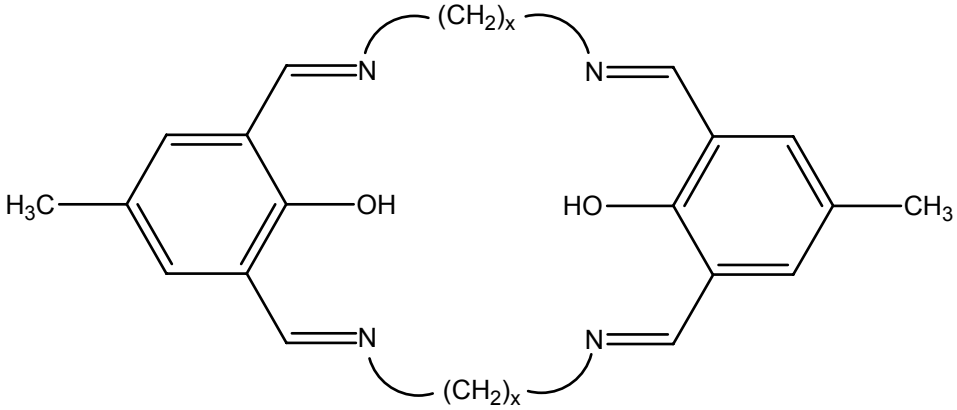

Figure 1.3: Example of a simple Robson Macrocycle

The fact that this Robson macrocyclic ligand was able to hold two metals in close proximity led to the possibility of developing these types of ligands as models for the active sites of metalloproteins.[10,3] Many biological catalysts have two or more metals in the active site. Examples of these are hemocyanin, methane monooxygenase, urease (figure 1.4) and the manganese cluster involved in the photosystem II (PSII) oxygen-evolving reaction in photosynthesis.[11-15] The study of small molecule analogues is important because active sites of enzymes are surrounded by a protein polymer and difficult to access. In terms of function, small molecule analogues are synthesized in an attempt to replicate and understand the mechanism of the enzyme.

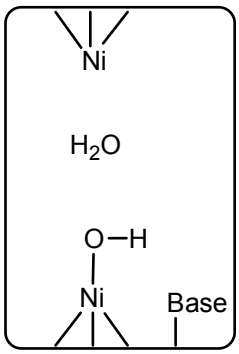

Figure 1.4: Model for the active site of Urease, which illustrates an enzyme with more than one metal present in the active site.

1.3 Compartmental Ligands

Fenton introduced the term "compartmental ligands" in 1977[16]. Compartmental ligands are dinucleating ligands and can be divided into three groups.[17] The first of these are macrocyclic ligands. The other two remaining groups are acyclic and can be subdivided into "end-off" and "side-off" ligands. These are also known as pendant-arm ligands. End-off ligands occur when a donor bridge is removed from the macrocycle resulting in one endogenous bridging site and one exogenous bridging site available between the two metals. Side-off ligands arise when one non-donor bridge is removed leaving two endogenous bridges accessible to the metal ions.

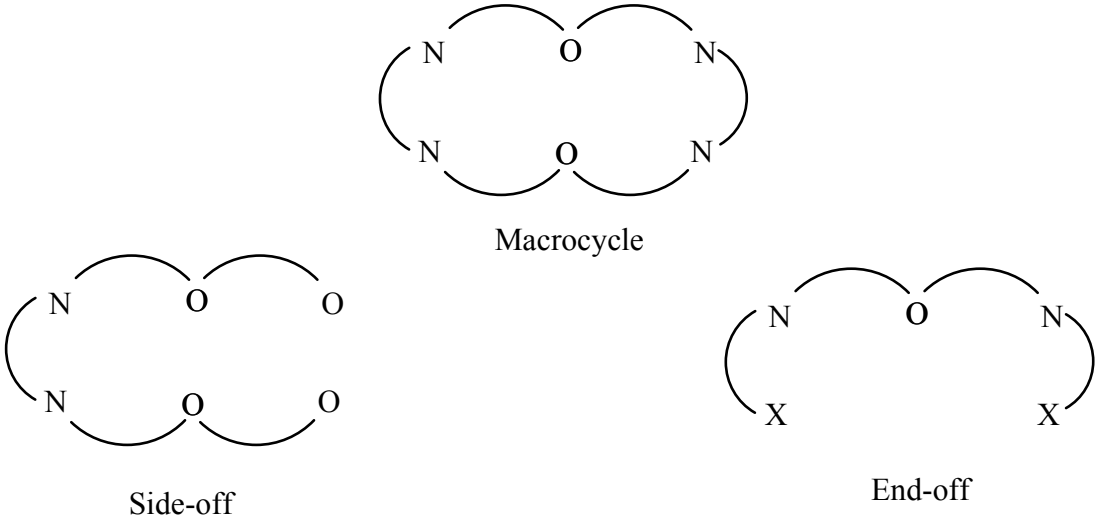

Figure 1.5: basic examples of different types of compartmental ligands

Acyclic compartmental ligands are good for mimicking enzymes because they are able to hold multiple metals in close proximity. However, end-off ligands also have enough flexibility to allow the metals to move away from each other if necessary. This is an advantage over traditional macrocycles, and their side-off counterparts, because these macrocycles have geometries which are rigid and somewhat compact.

1.3.1 Head units

Pendant-arm ligands are divided into two parts; the head-unit and the pendant arms. Commonly used head-units are dicarbonyl compounds, more specifically 2,6-disubstituted phenols. An example of this is DFMP. This is a widely used head-unit in macrocycles and acyclic ligands.[18-21,7,13,4] 5,5'-Di-tert-butyl-2,2'-dihydroxy-3,3'-methanediyl-dibenzene methanol (DHTMBA) is an extension of this head unit. This

has been used fairly extensively by McKee in pseudocalixarene macrocycles[8] and pendant arm ligands.[22]

1.3.1.1 DHTMBA

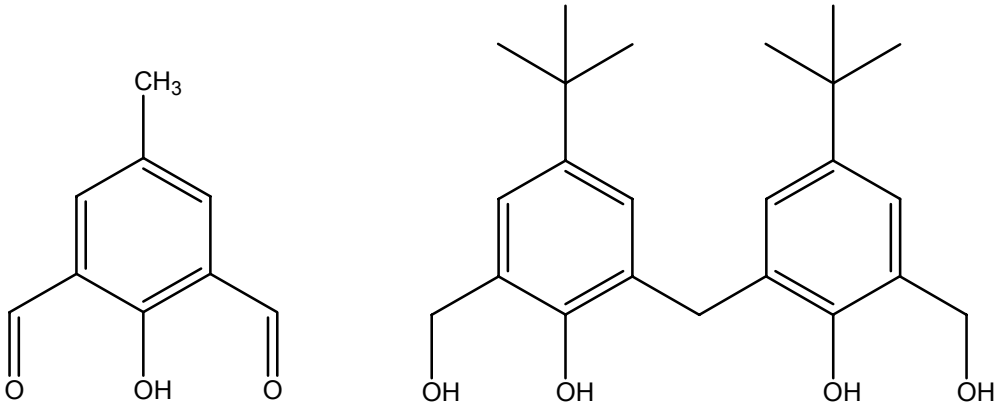

dfmp dhmtb

Figure 1.6: DFMP and DHTMBA head units

DHTMBA is an ideal head unit because it has flexibility in that it is able to rotate around the carbon atom which joins the two rings. There is also free rotation in the arms. There are two free phenol groups which creates uncertainty as to where and how the metals will bind. The inclusion of the two phenol groups makes it possible for the ligand to bind more than two metals.

1.3.2 Pendant Arms

There are many types of pendant arms (figure 1.7). Both symmetric and unsymmetric have been used. However, if biomolecular modelling is the intention, arms with biological relevance have an obvious advantage.

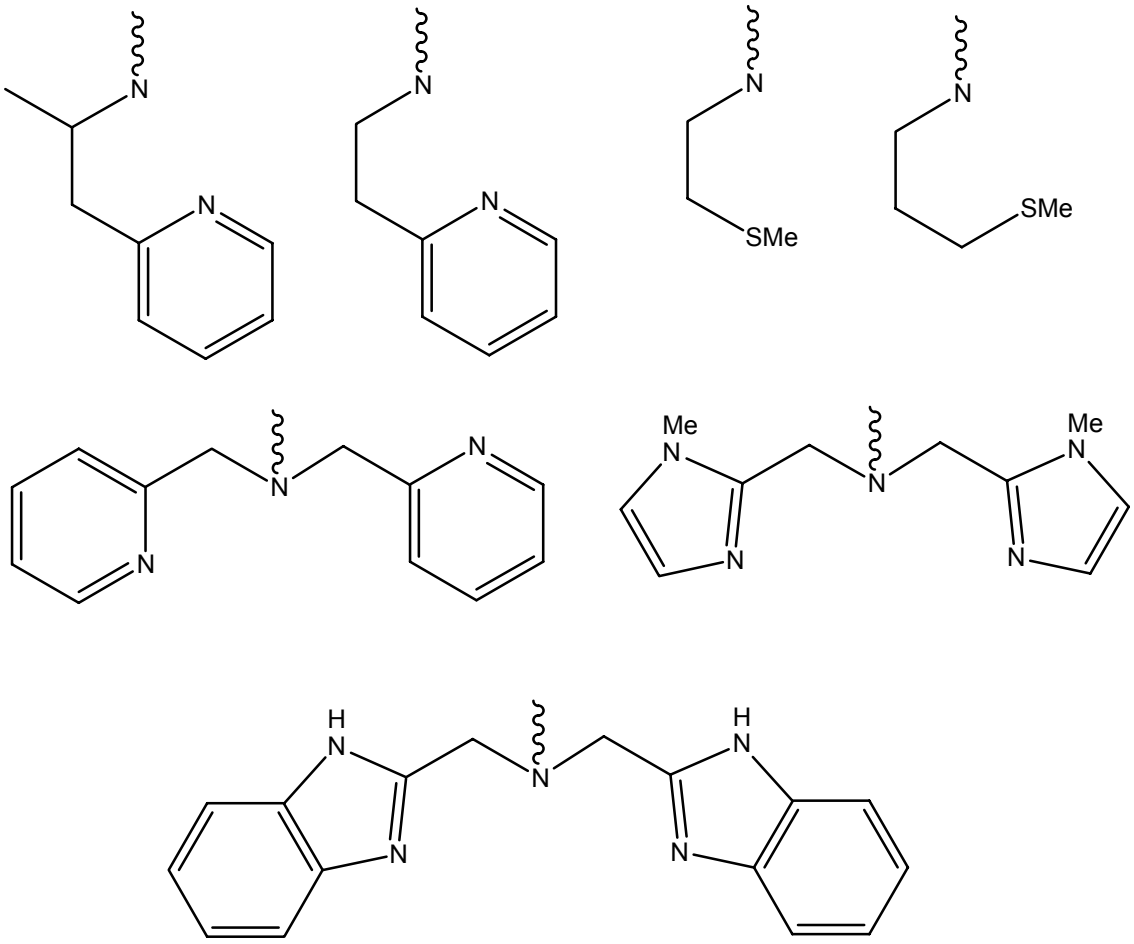

Figure 1.7: Examples of pendant arms. The bottom structure is Bis(benzimidazole-2-ylmethyl)amine (BBIM).

1.3.2.1 BBIM

The ligand, L1, (Figure 1.1) proposed in this study is an end-off compartmental ligand. Hence, it is a dinucleating ligand in which two separate donor areas exist. The head-unit consists of DHTMBA. The arms are bis(benzimidazole-2-ylmethyl)amine (BBIM). These have been chosen because they contain imidazole groups which have biological relevance in two different manners. The first of these is to do with inhibition of the yeast *Candida albicans.* Recent experiments have shown that metal complexes containing imidazole groups are effective in inhibiting the growth of the fungal yeast *Candida albicans.*[23,24] Overuse of drugs in present times has caused mutations in bacteria, fungi and viruses to occur more rapidly. When mutations take place the effectiveness of the drug designed to inhibit the disease can be compromised. This causes drug resistance. *Candida albicans* is a very common yeast

which causes many diseases.[24] This is why it is essential to create new drugs with new mechanisms of drug delivery. Metal complexes with imidazole groups have potential here.

The other more specific reason that the BBIM arms have biological significance is that the benzimidazole segment is very similar to part of the histidine side chain (figure 1.8) and many metal centres in enzymes are surrounded by histidines. A prime example of this is hemocyanin.

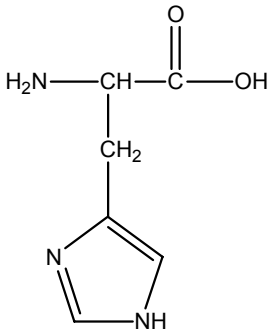

Figure 1.8: Part of the histidine side chain

1.4 Hemocyanin

Hemocyanin is a dioxygen transport protein present in the blood of several species of molluscs and arthropods.[25] Each hemocyanin active site has two copper ions which are able to bind one dioxygen.[26] In 1993 the crystal structure of hemocyanin in the horseshoe crab, *Limulus,*[27] became the accepted version as another crystal structure on the spiny lobster, *Panulirus interruptus*,[28] had unusual coordination around the copper(I) ions[25].

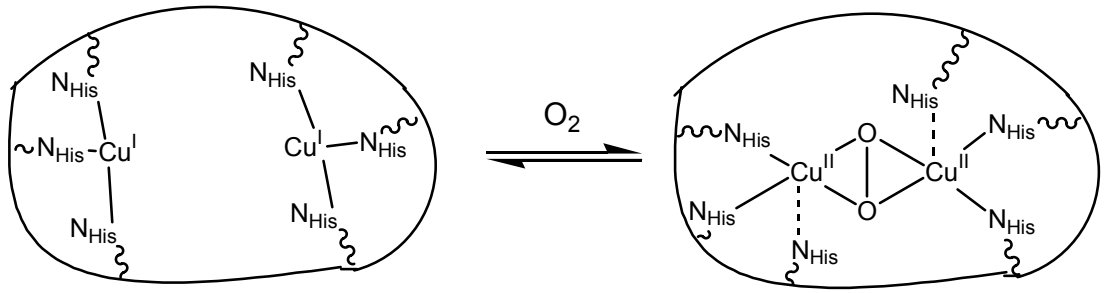

Deoxyhemocyanin Oxyhemocyanin

Figure 1.9: Structures of deoxy- and oxyhemocyanin from the horseshoe crab.

The crystal structure[27] showed that the Cu^{I}-Cu^{I} distance in deoxyhemocyanin was 4.6Å and the Cu^{II}-Cu^{II} distance after binding O_2 was 3.6Å. Thus a flexible molecule would better mimic the system than a macrocycle, which is capable of some conformational change but not a great amount due to a fairly defined shape. The copper ions were secured to the protein by histidines. Therefore, to attempt to mimic this reversible O_2 binding of hemocyanin, it would be advantageous to have histidine-like units present.

1.4.1 Complexes synthesized to mimic hemocyanin

In 1984 McKee *et al*[29] synthesized $[Cu_2(L\text{-}Et)(N_3)]^{2+}$ as a model for the active site of the dicopper(II) methemocyanin. This was a dinuclear copper(II) complex with ligands comparable to BBIM as the arms. They found it had similar geometry and magnetic properties as hemocyanin to the best of their knowledge because the first crystal structure of hemocyanin was not published until 1989.[28]

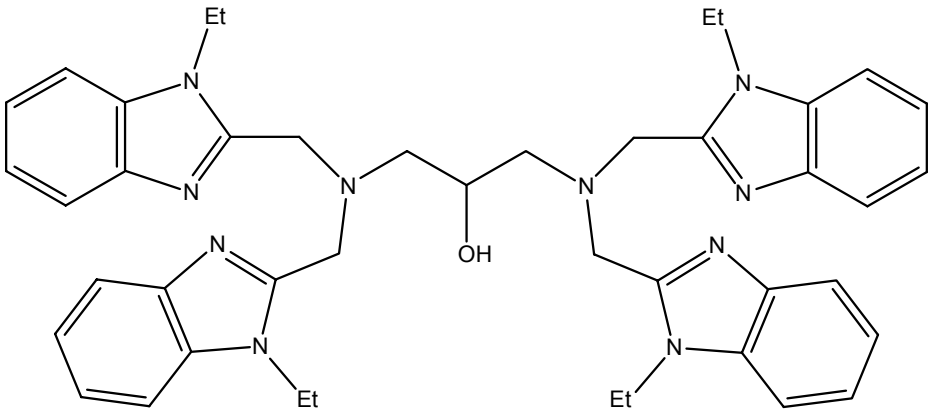

Figure 1.10: HL-Et

Consequently, in 1990 McKee *et al*[13] synthesized three dinuclear copper(I) compartmental complexes analogous to HL-Et (figure 1.10). The intention was to study the unusual coordination geometry which appeared around copper(I) in the crystal structure on the *Panulirus interruptus* deoxyhemocyanin.[30] McKee *et al* showed that the coordination around copper(I) can be highly distorted which was in agreement with the *Panulirus interruptus* data. However, some difficulty was encountered in that they were unable to reproduce the reversible O_2 binding. It was

concluded that this could be due to the fact that the ligands are not constrained enough. This is a potential problem with the ligand, L1.

1.4.1.1 Other complexes synthesized to mimic protein active sites

In 1988 Kolis[21] synthesized a similar ligand (HL-Im) with imidazoles, rather than benzimidazoles, as the arms. HL-Im was complexed with manganese to form a bidentate Mn(II,III) ligand. This was intended to represent a comparable coordination environment to several manganese proteins. Again, this is because several manganese proteins use histidine to attach the metal ion to the protein backbone: Examples are manganese superoxide dismutase, manganese catalase and the manganese centre of the oxygen-evolving complex involved in PSII in photosynthesis[14,31,32]. Thus these types of ligands have multiple uses for bioinorganic modelling. Since then there has been much more published on these types of proteins and there is a better understanding of their structures and mechanisms[33-41]. However, not everything is known so there is still a need for more models of the active sites to fully understand the mechanisms.

1.5 Synthetic Intentions

It was proposed to synthesize L1 from the head-unit, DHTMBA, with two equivalents of the pendant arm, BBIM, before complexing it with biologically-relevant metals such as copper and manganese. A similar ligand (Ln) (figure 1.11) has previously been synthesized by McKee and Fontecha[22] and complexed with copper. This group found Ln coordinated two copper ions and it has been proposed that L1 would coordinate similarly.

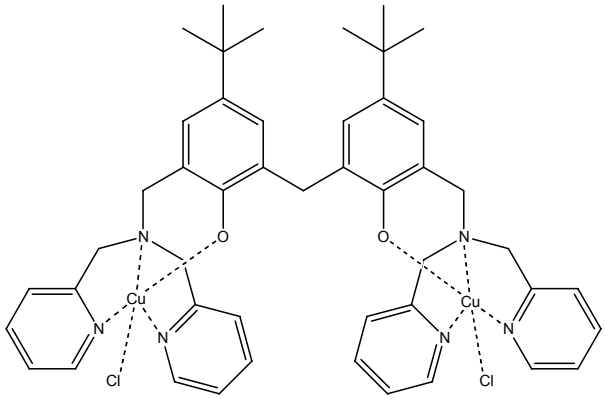

Figure 1.11: Cu_2LnCl_2 synthesized by McKee and Fontecha

Chapter 2

2 Crystallographic Studies

2.1 Introduction to Curtis Macrocycles

In 1961 Curtis and House proposed the first macrocyclic structure.[42] As a PhD student, while carrying out exchange rate reactions, Curtis needed to dissolve $Ni(en)_3^{2+}$ in acetone. $[Ni(en)_3][(ClO_4)_2]$ was dissolved in acetone and yellow crystals were obtained,[43] even though a purple solution was expected. This sufficiently bewildered Curtis that he attempted to determine the structure of the yellow crystals. In 1960 he first proposed (i) (figure 2.1) as the structure because he knew the product was diamagnetic and that all NH_2 groups had been eliminated.[44]

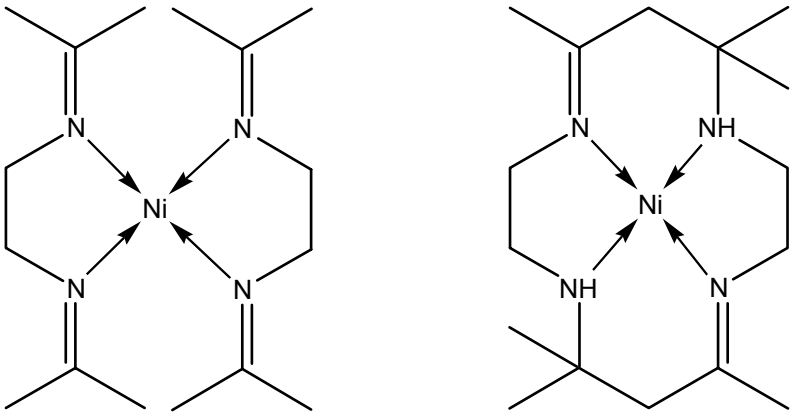

Figure 2.1: Proposed structures of macrocycles; (i) and (ii) respectively

However, the IR showed that there were still N-H bonds present so the compound was decomposed in cyanide. The only isolated compound from this was mesityl oxide (figure 2.2). From this, the structure was deduced to be that of (ii) (figure 2.1). The macrocycle consisted of four nitrogens, two amines and two imines, connected through two three-carbon bridges and two two-carbon bridges. The macrocycle formed so that the two-carbon bridges are opposite each other and so are the three-carbon bridges. The *trans* macrocycle, where the imines are diagonally opposite

(figure 2.1(ii)), was found to be the major product. The *cis*, where the imine nitrogen atoms are directly opposite, was found to be the minor. These azamacrocycles formed from the template reactions of acetone with metal-amine compounds are now called "Curtis Macrocycles".[10]

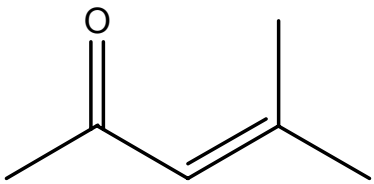

Figure 2.2: Mesityl Oxide

One of the most astonishing things in the creation of these macrocycles was the formation of bonds. Not only were there C—N single and double bonds formed but also new C—C bonds. The macrocycles are formed by connecting the metal diamines with a three carbon bridge produced from two acetone molecules (figure 2.3).[45]

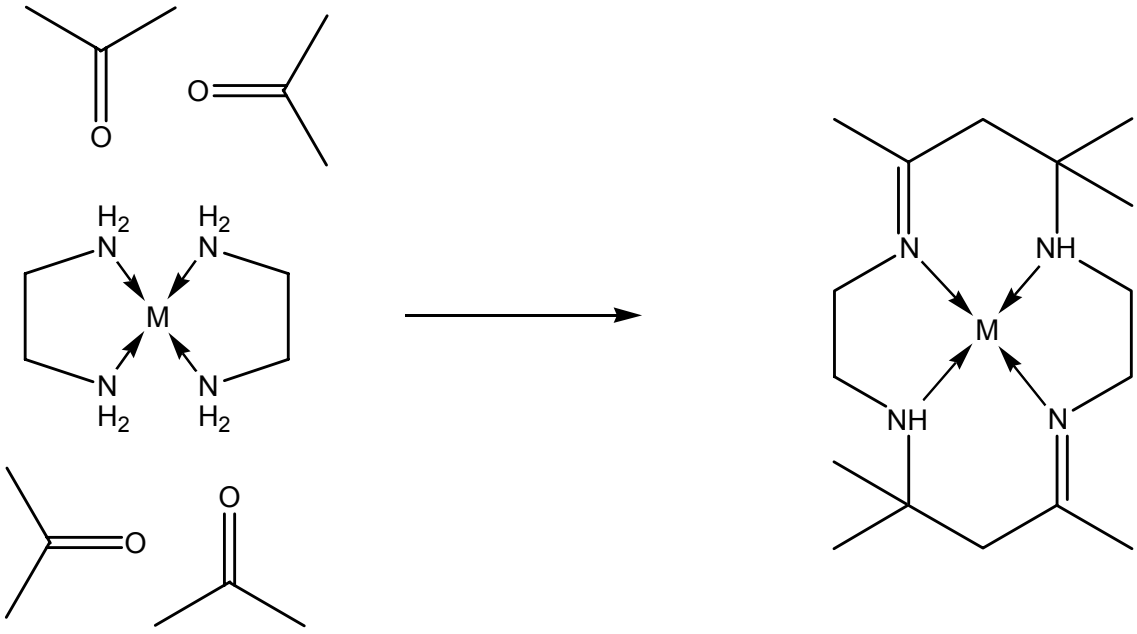

Figure 2.3: Formation of a Curtis Macrocycle[45]

2.2 Chapter Summary

This chapter summarizes the crystal structures of nine Curtis compounds. Initially they have been compared with each other and the important parts of each structure are highlighted. Each result is then described in further detail and tables comparing crystallographic data are provided for all the structures in the appendix. Each compound gets labeled with a particular code when they enter the X-ray laboratory. This usually does not have anything to do with the actual structure and the sole purpose is to make compound identification easier. During this chapter each compound will be referred to by their code name for ease of explanation.

X-ray crystallographic data were collected on either a Siemens CCD area detector or a Bruker Apex II using graphite monochromated Mo Kα (λ = 0.7107 Å) radiation. Crystals suitable for X-ray crystallography were mounted on a glass fibre using a hydrocarbon oil and transferred into a low temperature nitrogen stream. All data sets were collected at 93K unless the low temperature nitrogen stream was not operational. The temperature is presented in the crystallography tables in the appendix. The data were corrected for absorption using the multi-scan technique by the program SADABS.[46] The structures were largely solved by direct methods using SHELXS, but occasionally the Patterson vector method was employed. The model was then refined on F^2, using all data, by full-matrix least-squares procedures with SHELXL-97. All non-hydrogen atoms were refined with anisotropic displacement parameters. Hydrogen atoms were inserted at calculated positions using a riding model with thermal parameters equal to 1.2U or 1.5U of their carrier atoms, depending on the type of hydrogen atom.

2.3 Comparison of the Structures

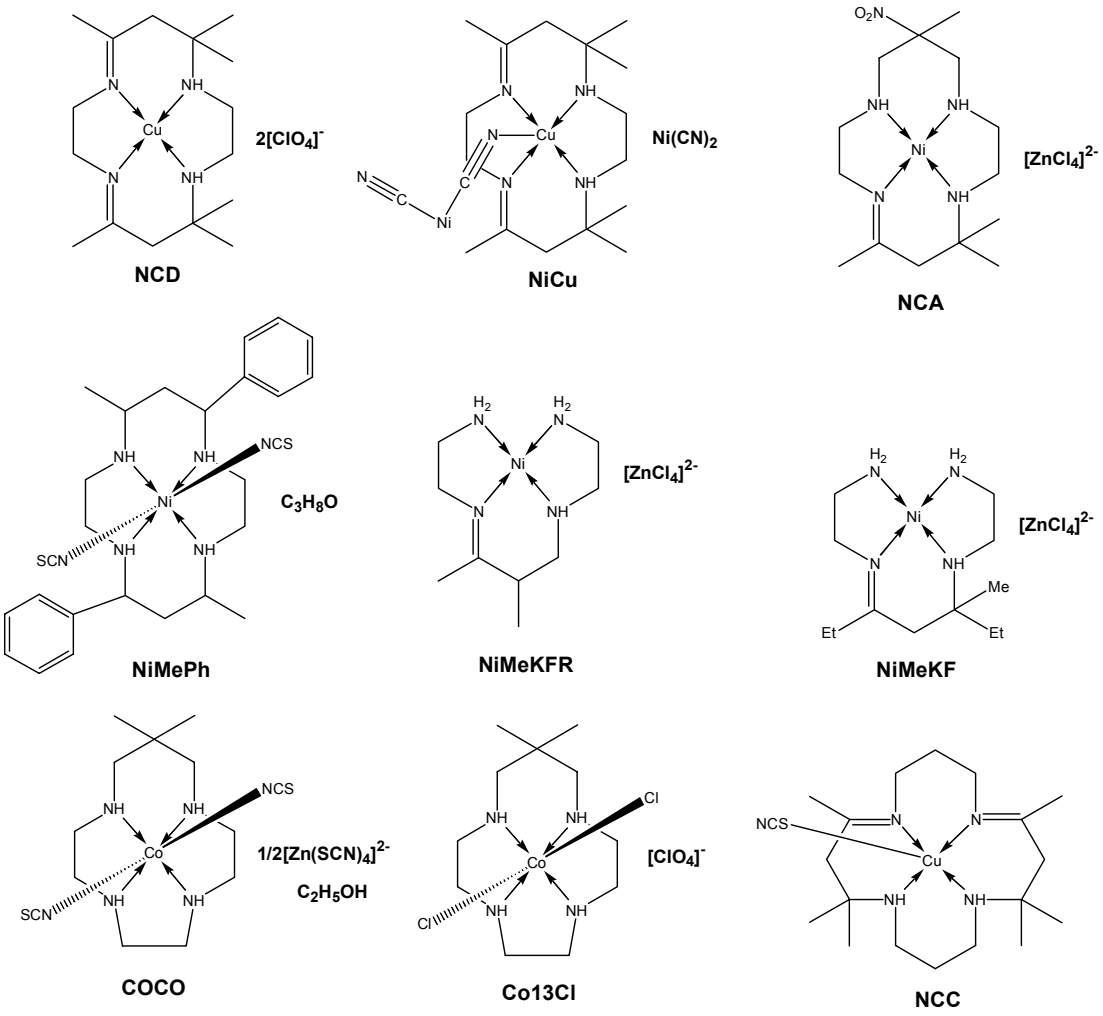

Figure 2.4: Structures of the nine Curtis macrocycles covered in this chapter

NCD[47,48] contains the standard Curtis macrocycle and is formed from the condensation reaction of acetone with ethylenediamine copper(II). The main distinguishing factor is that it is the *cis* form, the minor product in these types of reactions. Ni(II) and Cu(II) are the only metals that will form the *cis* isomer from this reaction.[49] NiCu[47] is the same compound as NCD with a different anion. The anion, tetracyanonickelate(II) is joined to the copper(II) through a nitrogen atom. NCA[50] differs from the previous two structures in that it has only one imine nitrogen atom. The synthesis involves $Ni(en)_2$ reacting with two equivalents of acetone (rather than four in the cases of NCD and NiCu) which creates a structure similar to NiMeKF.

However all terminal groups are methyl groups rather than ethyl. This NiMeKF-like structure was then reacted with nitroethane and paraformaldehyde to give NCA.[50]

NiMeKF and NiMeKFR[51] are not complete macrocycles as they lack a second three-carbon bridge to complete the structure. These compounds were formed by the reaction of $[Ni(en)_3][ZnCl_4]$ in 2:1 methanal:butanone with paraformaldehyde.[52] Both these structures are formed in the same reaction and are separated by crystallization. NiMeKF is analogous to NCD without the second three-carbon bridge. The reaction of two moles of butanone causes the inclusion of ethyl groups, whereas NiMeKFR is formed by the reaction of methanal and butanone which creates two methyl groups on the three-carbon bridge (figure 2.5).

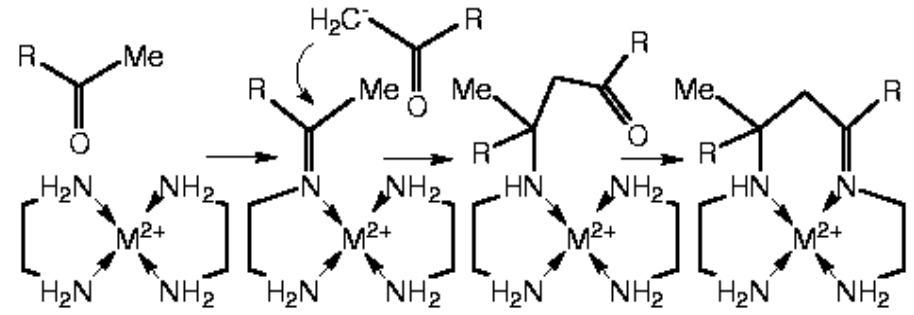

(a)

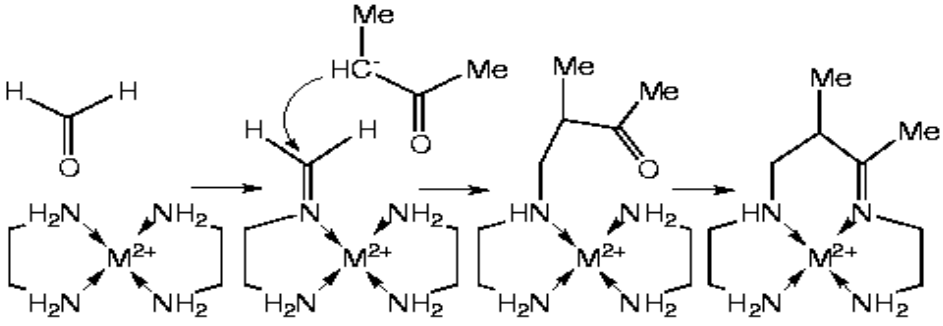

(b)

Figure 2.5: Reaction schemes[50] showing (a) the formation of NiMeKF, where R=Et, (b) the formation of NiMeKFR

NiMePh is a standard nickel Curtis macrocycle where the imines have been reduced so all four nitrogens are amines. When Curtis macrocycles are synthesized they initially form diimine complexes (figure 2.3). To get a tetraamine complex the macrocycles must be reduced, usually with $NaBH_4$.[53] This creates stereochemical

centres at the carbon atoms that have been reduced.[43] In NiMePh there is disorder at these carbon atoms so it is impossible to distinguish the stereochemistry. NiMePh has two axial thiocyanate ligands which are coordinated through the nitrogens. There is a methyl group and a phenyl ring substituent, on C1 and C3 respectively, on both three-carbon bridges in a *trans* arrangement.

COCO and Co13Cl are cobalt macrocycles with similar structures. The key difference is that COCO has thiocyanate ligands in the axial positions and Co13Cl has chlorine atoms. They also have different counter-ions. COCO and Co13Cl differ from the other structures because they have only one three-carbon bridge and they have three two-carbon bridges. They both have four amine nitrogens and on the central carbon on the three-carbon bridge there are two methyl groups.

NCC is the only compound which has four three-carbon bridges. Two of the three-carbon bridges have no substituents and two have dimethyl groups on C1 and C3 of their bridges. This copper(II) macrocycle is symmetrical so that the opposite three-carbon bridges are the same. There is one axial thiocyanate ligand which creates a bowl-type structure (figure 2.11).

2.4 NCA: (5,7,7,13-tetramethyl-13-nitro-1,4,8,11-tetraazacyclo-tetradec-4-ene)-nickel(II) tetrachlorozincate

This compound, $C_{15}H_{33}N_5NiO_2.ZnCl_4$, was solved in the monoclinic space group $P2_1/n$ and refined to 3.5%. It contains a central Ni(II) ion which has a square planar coordination to four nitrogens. Three of the nitrogens are secondary amine nitrogens; N1, N8 and N11, and the fourth is an imine, N4. The asymmetric unit contains one cation and one tetrachlorozincate counter-ion (figure 2.6).

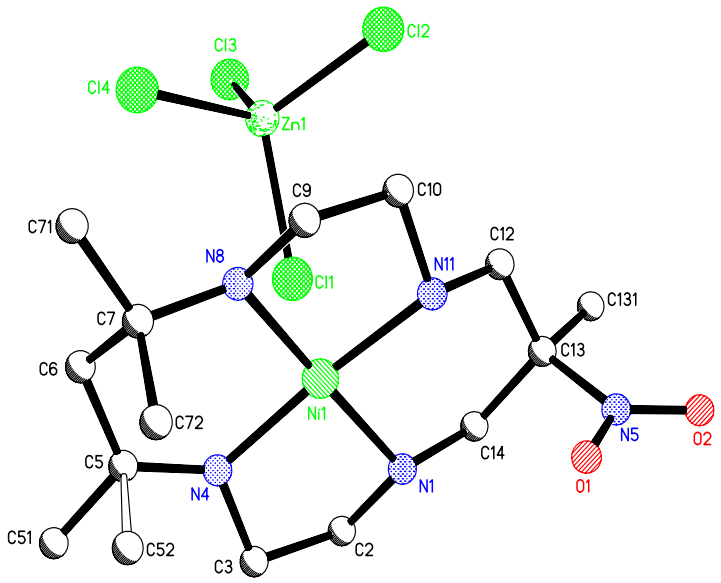

Figure 2.6: Diagram of the asymmetric unit of NCA consisting of one macrocycle and one tetrachlorozincate anion. C52 has a white bond to illustrate that it is a disorder peak. Hydrogen atoms have been omitted for clarity.

The model has a pseudo internal mirror plane running through C6, Ni1, C13, C131 and all atoms, O1, O2, N5, of the nitro group. There is disorder resulting from the nitrogens N4 and N8 both having imine character. This was modeled by the addition of C52 and H4, which is the hydrogen atom on N4. N4 is the imine 80% of the time; therefore C72 and H8, which is the hydrogen attached to N8, are present at 80% as well. N8 is the imine 20% of the time, so it follows that C52 and H4 are present 20% of the time. This is supported by the bond length of N4—C5 being significantly shorter than of N8—C7 at 1.318(4)Å and 1.451(4)Å respectively. The N8 bond length is still noticeably shorter than those from N1 and N11 which are 1.472(3)Å and 1.479(4)Å respectively.

There is intramolecular hydrogen bonding between O1 of the nitro group and the amine hydrogens H1 and H11 (figure 2.7). There are also very weak hydrogen bonds between the chlorines of the tetrachlorozincate anion and the amine hydrogens, which create a three dimensional network with the anions sitting in between the layers of the macrocyclic complexes. A weak interaction is observed between Ni1 and Cl1 of the tetrachlorozincate anion with the distance between them being 2.921Å.

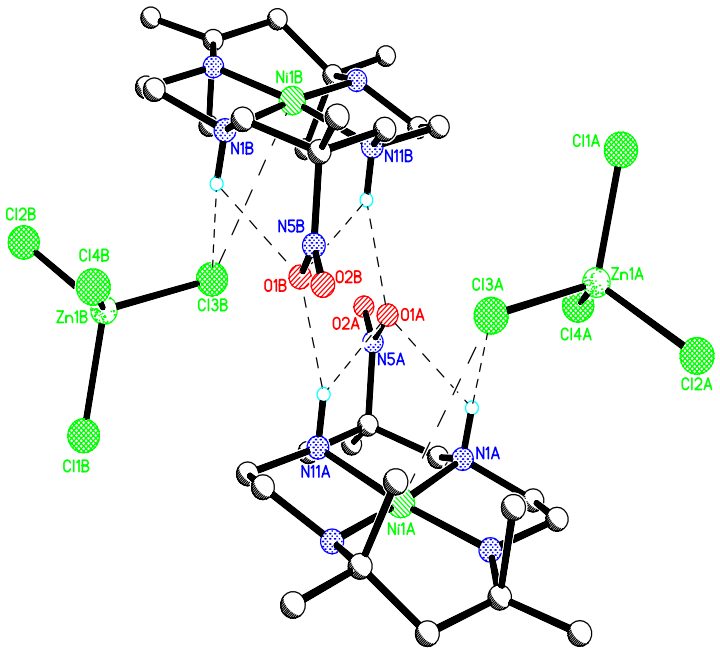

Figure 2.7: Part of the packing diagram of NCA showing the hydrogen bonding between the tetrachlorozincate anions and the macrocyclic complexes.

2.5 Co13Cl: (3,3-dimethyl-1,5,8,11-tetraazacyclotridecane) dichlorocobalt(III) perchlorate

The title compound, $C_{11}H_{26}N_4Cl_2.ClO_4$, was solved in the monoclinic spacegroup $P2_1/c$ and refined to 2.6%. Co13Cl contains a centrally located Co(III) which has octahedral coordination to four amine nitrogens; N1, N5, N8 and N11, and two chlorine atoms, Cl2 and Cl3, which are *trans* to each other. The asymmetric unit contains one macrocycle and one $[ClO_4]^-$ anion (figure 2.8).

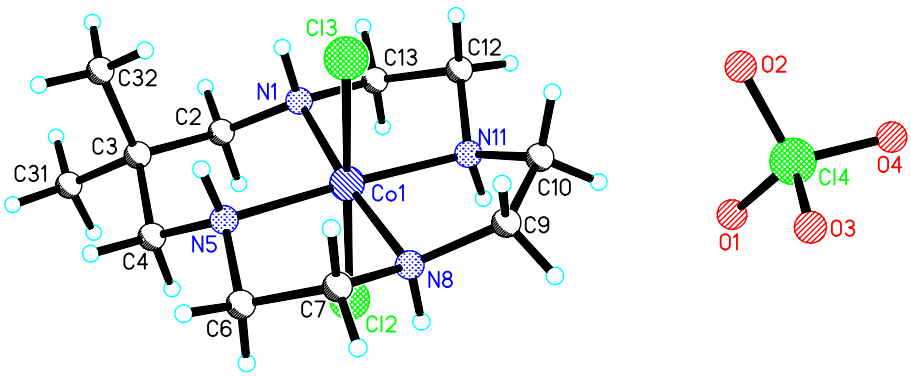

Figure 2.8: Diagram of the structure of the asymmetric unit of Co13Cl consisting of one macrocycle and one perchlorate anion.

Hydrogen bonding between the amine nitrogen atoms on the macrocycle and the perchlorate oxygen atoms creates a three dimensional lattice. The perchlorate anions are stacked between layers of macrocycles. Each cobalt macrocycle is hydrogen bonded to the oxygen atoms on three different perchlorate molecules. (figure 2.9). One individual perchlorate molecule binds to three different macrocycles between the layers.

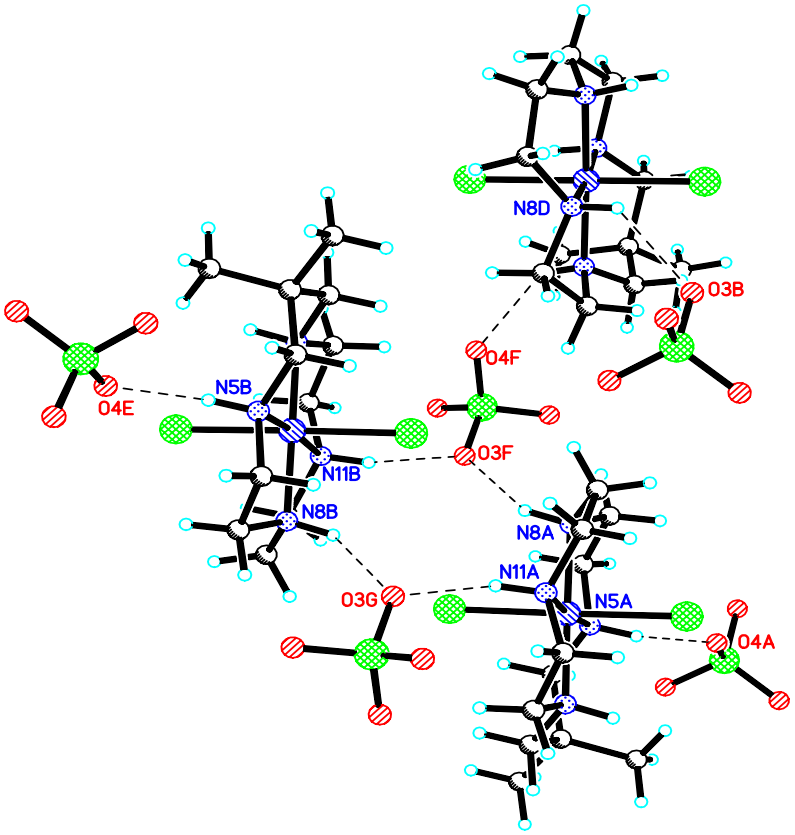

Figure 2.9: Structure of part of a packing Co13Cl showing the intramolecular hydrogen bonding between the Co13Cl macrocycle and perchlorate anions.

The bonds from Co1 to N8 or N11, at 1.9211(10)Å and 1.9187(10)Å respectively, are shorter than those bonds from Co1 to N1 or N5, at 1.9465(9)Å and 1.9429(10)Å respectively. This is due to N1 and N5 being incorporated in a 6-membered chelate ring within the macrocycle whereas N8 and N11 are part of 5-membered chelate rings.

2.6 NCC: (2,4,4,10,10,12-octamethyl-1,5,9,13-tetraazacyclo-hexadeca-1,11-diene)-isothicyanatocopper(II) perchlorate

NCC was solved in the orthorhombic space group Cmca and refined to 7.2%. This compound has a centrally-located copper(II) ion with square pyramidal coordination to two amine and two imine nitrogens in basal positions and one linear thiocyanate ligand in the apical position. The macrocycle has a crystallographic mirror plane so that the methyl and dimethyl groups are *cis* with respect to each other and hence the imine groups are *cis* with respect to each other. Only half the macrocycle constitutes the asymmetric unit, which also contains one half of a highly disordered perchlorate anion. Overall the macrocycle has a bowl shape.

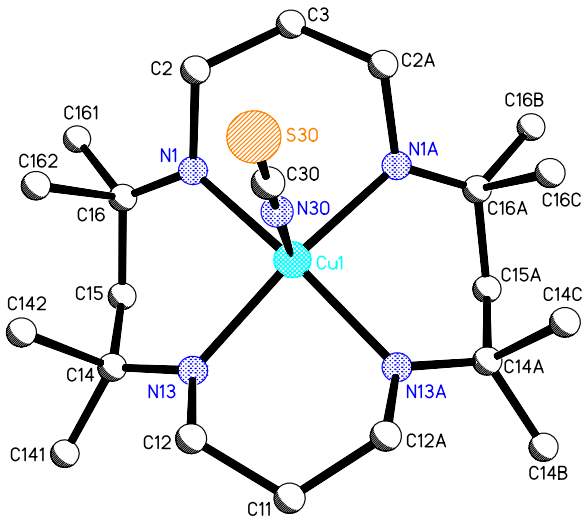

Figure 2.10: Structure of NCC showing the disorder peaks C162 and C16C at C16 and C16A respectively. Solvate molecules and hydrogen atoms have been omitted for clarity.

There is disorder located at C16. This was modeled by the addition of C162 which has the effect of reversing the chelate ring N1=C16(Me)—C15—C14(Me)$_2$—N13 to give N13=C14(Me)—C15—C16(Me)$_2$—N1. The site occupancy factors, of 0.59 and 0.41, show the first conformation; with C16 as the imine and C14 as the amine, is preferred over C16 being the amine and having the extra methyl group, C162, attached. This is emphasized by the lengths of the C—N bonds being 1.312(9)Å for N1-C16 which is shorter than the corresponding N13-C14 bond of 1.369(9)Å.

Very weak intermolecular hydrogen bonding between the sulfur atom of the thiocyanate and the amine hydrogen atoms creates a three dimensional lattice. Each sulfur atom is hydrogen bonded to the amine hydrogen atoms so that two central macrocycles are layered on top of one another. Another two macrocycles, on either side, are rotated 90° with their thiocyanate ligands pointing towards the central macrocycles. Throughout the structure there are distinct layers of macrocycles with the perchlorate anions sitting in between (figure 2.11).

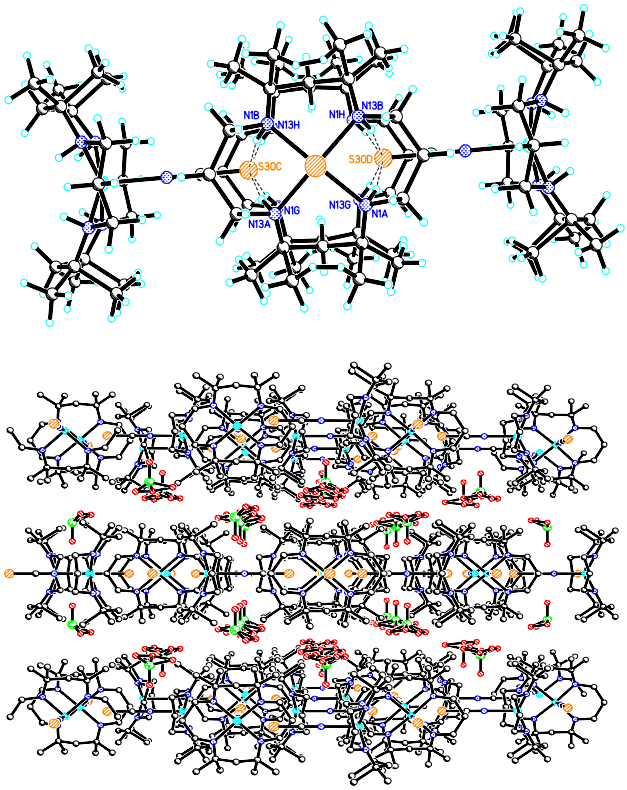

Figure 2.11: Pictures of NCC showing (a) part of one macrocycle layer in the unit cell and (b) a packing diagram illustrating the separate layers.

It is also possible to consider the macrocycles as a paddlewheel formation, where one thiocyanate is hydrogen bonded to the amine hydrogen atoms of another macrocycle, which in turn is hydrogen bonded through its thiocyanate sulfur atom to another macrocycle and so on until a square is formed (figure 2.12). Two disordered perchlorate anions sit in the cavity of this square.

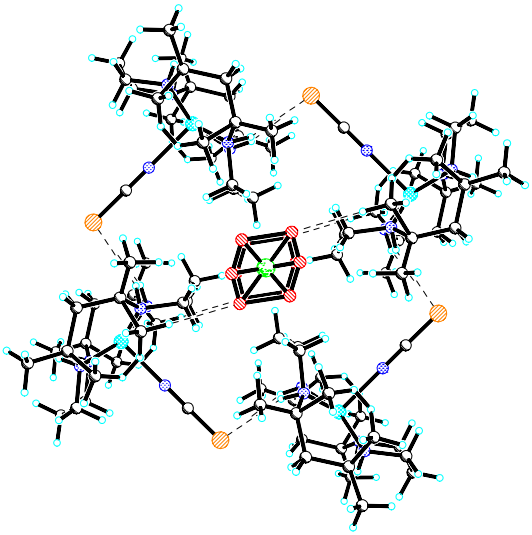

Figure 2.12: Packing diagram of NCC illustrating the paddlewheel formation of macrocycles with highly disordered perchlorate anions in the cavity.

2.7 NCD: N-rac-(5,5,7,12,14,14-hexamethyl-1,4,8,11-tetraaza-cyclotetradeca-7,11-diene)copper(II) perchlorate

The title compound, $C_{16}H_{32}N_4.2[ClO_4]$ was solved in the orthorhombic space group Pbcn. It contains a centrally-located copper(II) ion bonded in a square planar arrangement to two imine nitrogens; N8 and N11, and two amine nitrogens; N1 and N4. The macrocycle has a crystallographic 2-fold symmetry axis which runs through Cu1 and the centre of the bonds C2—C3 and C10—C9. Hence the imine nitrogen atoms are located *cis* with respect to each other within the macrocycle (figure 2.13). The asymmetric unit consists of one half of the macrocycle and one perchlorate anion.

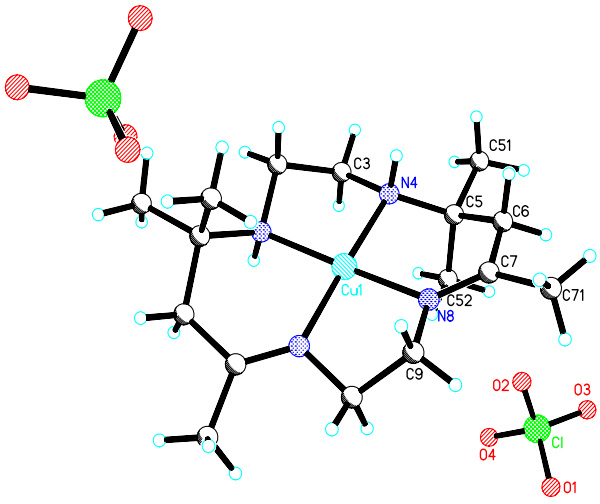

Figure 2.13: Diagram of NCD showing one macrocycle and two perchlorate anions

Within the unit cell there are separate layers of the macrocycles interspersed with the anions. The layers extend in two directions so that there are individual groups within each layer (figure 2.14(a)). Weak hydrogen bonding of the perchlorate oxygens; O1 and O4, and the amine hydrogen atoms link the different layers. There is also a weak interaction between O4 and Cu1 of 2.969Å that links the macrocycles and the perchlorate anions within the layers (figure 2.14(b)).

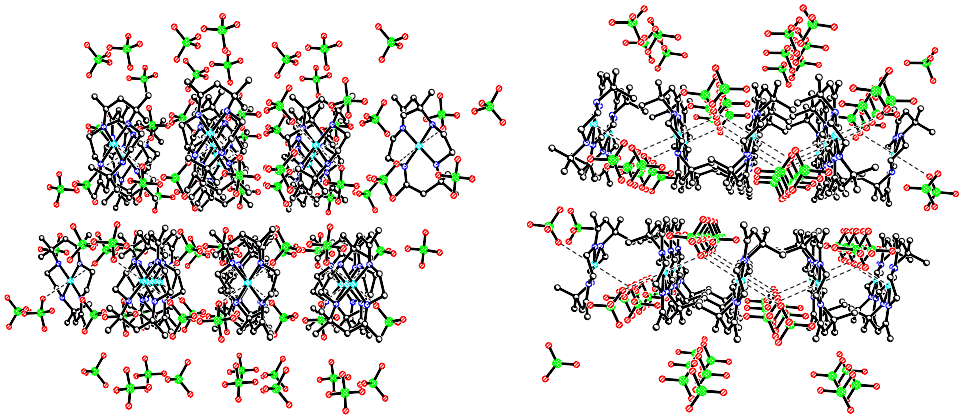

Figure 2.14: Packing diagrams of NCD illustrating (a) the distinct layers within the unit cell and (b) the weak interactions that link the molecules within individual layers

2.8 NiCu: Di-μ-cyano-1:2κ2 C:N;1:3κ2 C:N-dicyano-1κ2 C-bis-(N-rac-5,7,7,12,12,14-hexamethyl-1,4,8,11-tetraazacyclo- tetra deca-4,1 (14)-diene)copper(II)-nickel(II) tetra cyano-κ1 C) nickelate(II)

This structure has the same macrocyclic cation as NCD but the anion is a square-planar tetracyanonickelate ion. NiCu was solved in the triclinic space group P-1 and refined to 2.8%. The macrocycle contains a centrally-located copper(II) ion bound in distorted octahedron coordination to two imine nitrogens; N1 and N4, and two amine nitrogens; N8 and N11. The copper(II) sits on a centre of inversion which runs between the centre of the bonds C2—C3 and C10—C9. The nickel atoms; Ni2 and Ni3, are on centres of symmetry and so the asymmetric unit contains one copper macrocycle and two half nickel anions, with one half bound through N30 to the copper(II) ion with a bond distance of 2.2979(19)Å (figure 2.15).

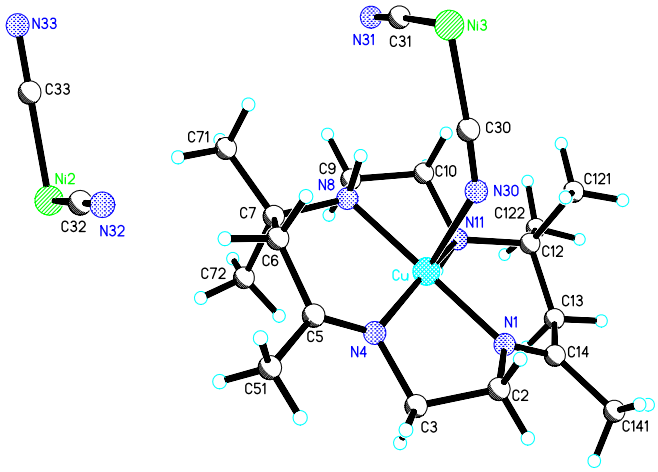

Figure 2.15: The asymmetric unit of NiCu illustrating the coordination of a half tetracyanonickelate to the copper macrocycle. Hydrogen atoms have been omitted for clarity.

The bound tetracyanonickelate anion bridges two macrocycles together so the Cu--Cu distance is 9.919Å (figure 2.16). The two connected macrocycles are related by an inversion centre. The nitrogens; N32 and N33, on the other anion are weakly hydrogen bonded to the amine hydrogen atoms; H8 and H11, on the macrocycle which creates individual layers of macrocycles with the anions and gives the impression of a grid in the packing diagram (2.16(b))

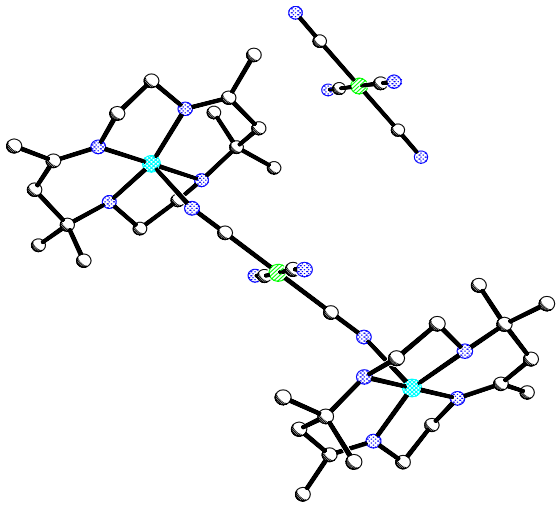

(a)

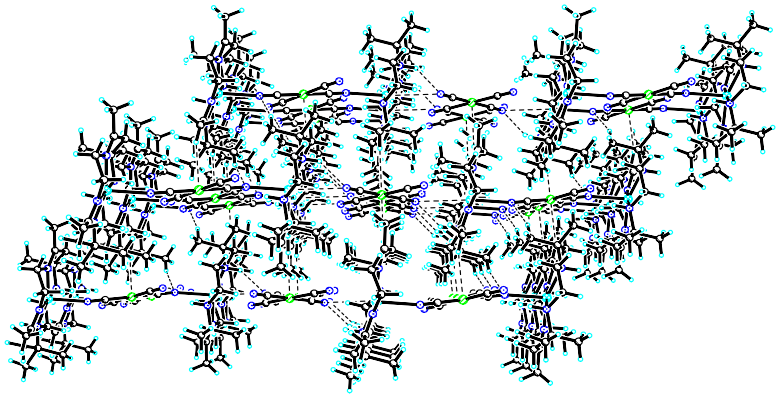

(b)

Figure 2.16: Pictures of NiCu showing (a) how a tetracyanonickelate anion bridges two macrocycles. Hydrogen atoms have been omitted for clarity. (b) the grid-like packing of the macrocycles.

2.9 NiMeKF: 6SR,7RS-(4,6-diethyl-6-methyl-3,7-diazanon-3-ene-1,9-diamine)nickel(II) tetrachlorozincate

The title compound, $C_{12}H_{28}N_4Ni.ZnCl_4$, was solved in the tetragonal space group $P4_12_12$ and refined to give a value of 3.1%. NiMeKF has a centrally-located Ni(II) in square planar coordination with three amines and one imine. The imine N=C bond length of 1.275Å is shorter than that of the corresponding amines with their respective carbon atoms, as expected. The N7—C6 bond length of 1.496(3)Å is the only bond length that is strictly comparable to the N3=C4 double bond because N1 and N9 lack the three-carbon bridge. The bond lengths show, without a doubt, that N3 is the imine nitrogen atom. The counter-anion is $ZnCl_4^{2-}$. NiMeKF is not a 'traditional' Curtis macrocycle because it lacks one three-carbon bridge, as previously stated. This results in only two two-carbon bridges and one three-carbon bridge with ethyl groups on C4 and C6 and a methyl group on C6 (figure 2.17).

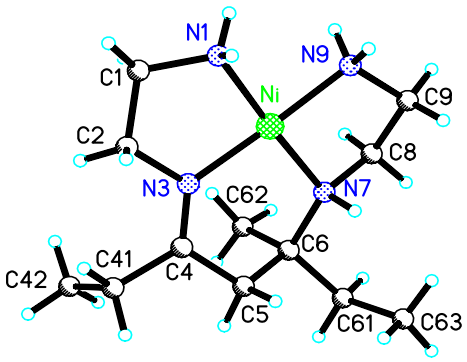

Figure 2.17: Diagram of the structure of NiMeKF illustrating that there is only one three-carbon bridge. $ZnCl_4^{2-}$ anion has been excluded for clarity.

The packing diagram shows a 3D network of layers of NiMeKF macrocycles with tetrachlorozincate anions within the unit cell (figure 2.18). This means that there are several layers within the unit cell as opposed to only one layer of macrocycles in each unit cell.

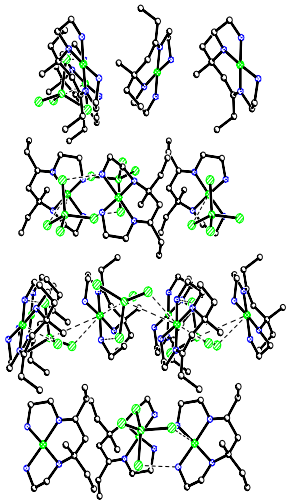

Figure 2.18: Packing diagram showing layers of the macrocyclic cations with tetrachlorozincate anions. Hydrogen atoms have been omitted for clarity.

2.10 NiMeKFR- 5SR,7RS-(4,5-dimethyl-3,7-diazanon-3-ene-1,9-diamine)nickel(II) tetrachlorozincate

NiMeKFR was solved in the orthorhombic space group $Pna2_1$ and refined to 2.4%. As stated previously NiMeKF and NiMeKFR are formed in the same reaction. In NiMeKFR the centrally located Ni(II) is coordinated to three amine nitrogens; N1, N7

and N9, and one imine nitrogen, N3, in a square-planar arrangement. The N=C imine bond of 1.289(3)Å is significantly shorter than that of the associated N—C amine bond which is 1.484(3)Å. There is a methyl group on two of the carbons; C4 and C5, of the three-carbon bridge. The asymmetric unit contains one macrocyclic cation and one tetrachlorozincate anion (figure 2.19).

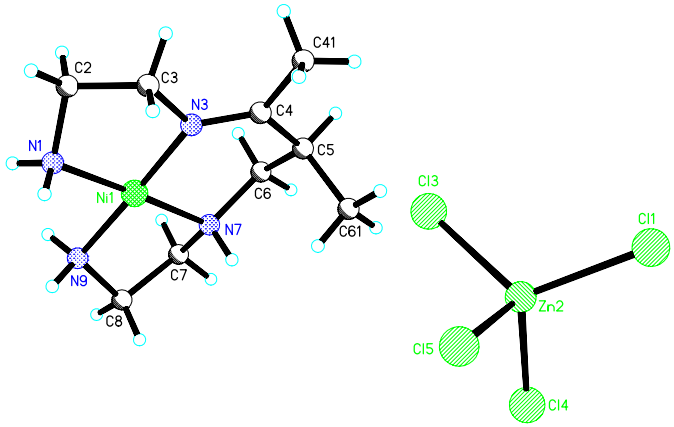

Figure 2.19: Diagram of the asymmetric unit of NiMeKFR, consisting of one NiMeKFR macrocycle and one tetrachlorozincate anion.

The packing diagram shows there are no particularly clear layers of either macrocycles, anions or both macrocycles with anions. It appears to show hydrogen bonding between the amine hydrogen atoms and the chlorine atoms from the tetrachlorozincate anions (figure 2.20). However the lengths of the bonds range from 2.39Å—2.94.Å, so it is highly unlikely that this is real hydrogen bonding.

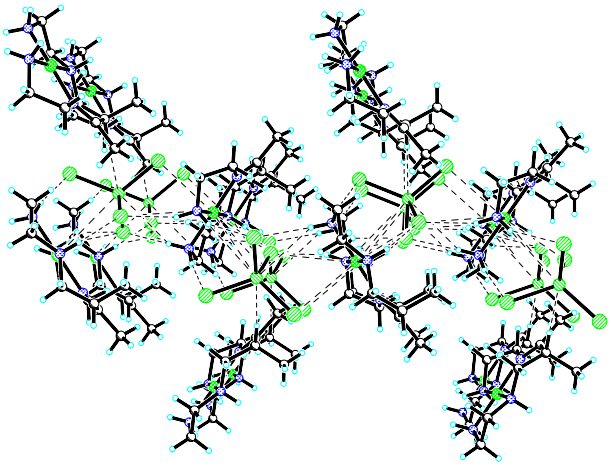

Figure 2.20: Packing diagram of NiMeKFR illustrating how the macrocycles do not form clear layers within the unit cell as opposed to other structures such as NCD.

2.11 NiMePh: (5,12-dimethyl-7,13-diphenyl-1,4,8,11-tetraaza-

cyclotetradecane) diisothiocyanatonickel(II) acetone solvate

The title compound was refined to 7.2% and solved in the monoclinic space group $P2_1/n$. NiMePh has a centrally-located Ni(II) ion in an octahedral arrangement to four amine nitrogens; N1, N1A, N4 and N4A, and two bent thiocyanate ligands *trans* with respect to each other. The asymmetric unit contains two half macrocycles, with the nickel(II) ions on different centres of symmetry, and one acetone solvate molecule (figure 2.21). There is a terminal phenyl ring on each C7 and C7A. The angle of the mean plane of the phenyl groups to the mean plane of the macrocycle is 75.88˚ (figure 2.22).

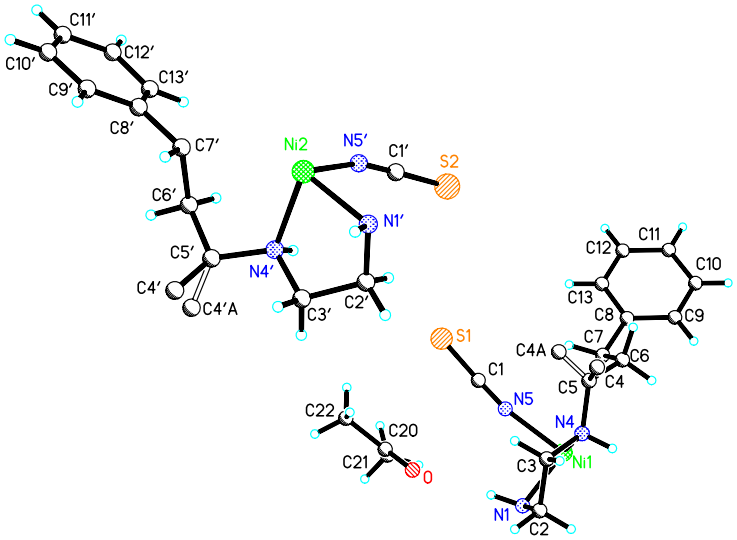

Figure 2.21: Diagram illustrating the constituents of the asymmetric unit of NiMePh; two half macrocycles and one acetone solvate molecule.

There is a centre of inversion through the nickel(II) ion (figure 2.22). Disorder is observed at C5 and C5'. The terminal methyl groups, in both independent macrocycles, are disordered over two tetrahedral sites. This was modeled by the addition of the peaks C4A and C4'A respectively. The site occupancy factors of 0.60 and 0.40, for C4 and C4A respectively, show that C4 is the major component in this macrocycle. However, in the other macrocycle C4' is the minor component with a site occupancy factor of 0.46.

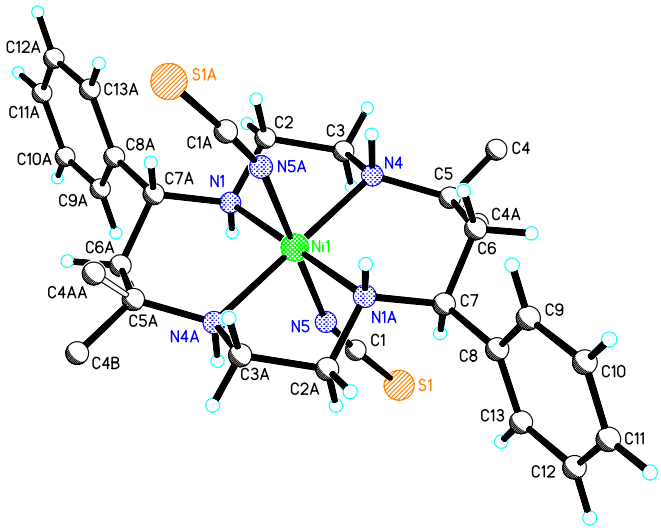

Figure 2.22: Diagram of the structure of one NiMePh macrocycle showing the disorder at C5 and C5A. Notice that the phenyl rings are rotated 75.88˚ with respect to the macrocycle.

The packing diagram shows that the macrocycles align so that they are in distinct layers (figure 2.23). The bond lengths between the amine hydrogen atoms with either the oxygen atom from acetone or the sulfur atoms from another macrocycle, range from 2.45Å-2.62Å. These values indicate it is highly doubtful that any hydrogen bonding exists because they are much too large.

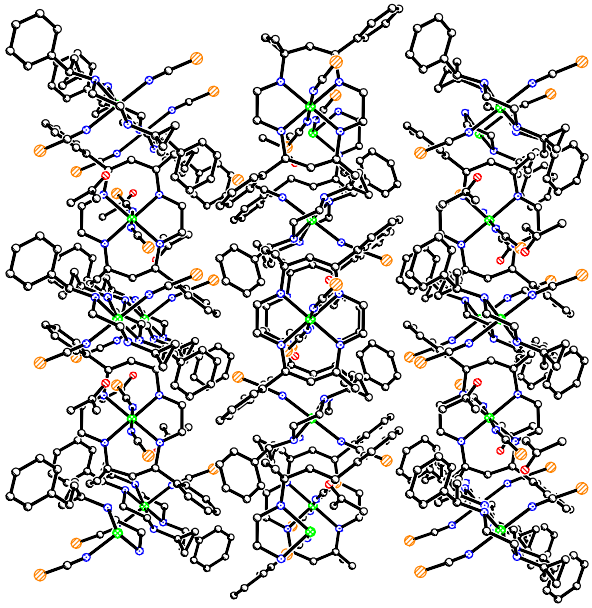

Figure 2.23: Packing diagram of NiMePh illustrating the layers of macrocycles

2.12 COCO: *trans*-(12,12-dimethyl-1,4,7,10-tetraazacyclo-tetradecane)diisothiocyanaocobalt(III) tetraisocyanatozinc(II) ethanol solvate

COCO was solved in the triclinic space group P-1 and refined to 1.9%. The macrocyclic structure contains a centrally-located Co(II) ion in an octahedral arrangement to four amine nitrogen atoms and two thiocyanate ligands, which are *trans* with respect to each other. Of the two thiocyanate ligands on each macrocycle one is linear and the other is bent. The asymmetric unit contains two macrocyclic cations, one tetrathiocyanozincate anion and one ethanol solvate molecule (figure 2.24).

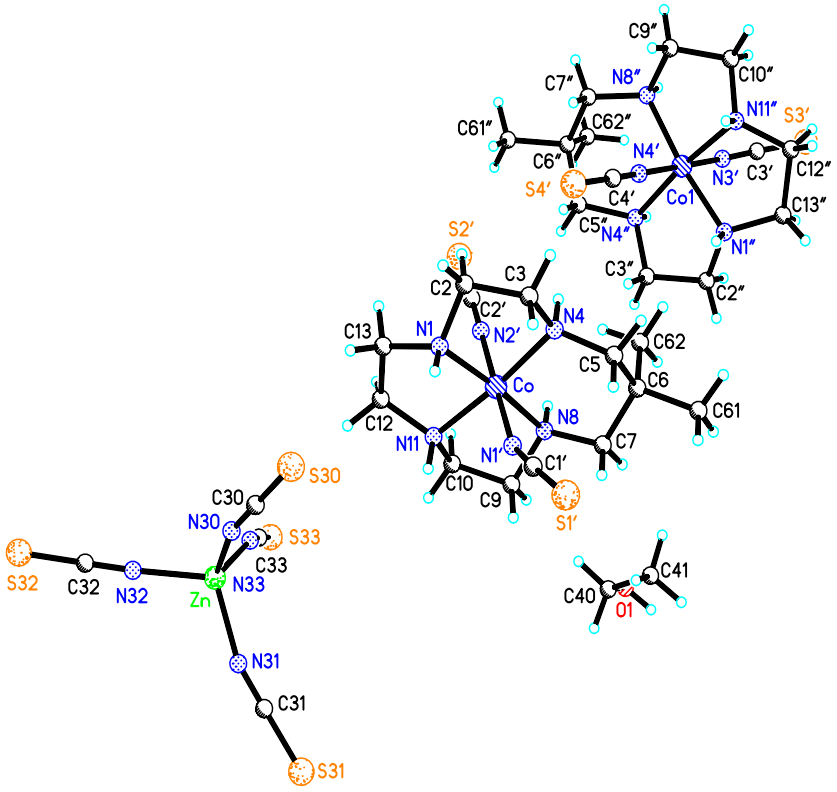

Figure 2.24: Diagram of the asymmetric unit of COCO consisting of; two cobalt(II) macrocycles, one tetrathiocyanozincate anion and one ethanol solvate molecule.

There is definite hydrogen bonding between amine hydrogen, H1', and the oxygen atom from the ethanol molecule with the H—O bond being 2.18Å. The distances between the thiocyanate sulfur atoms and the amine hydrogen atoms are all greater than 2.5Å so it is unlikely that these are forming hydrogen bonds. The packing

diagram of COCO shows a three dimensional network with no distinctive layers (figure 2.25).

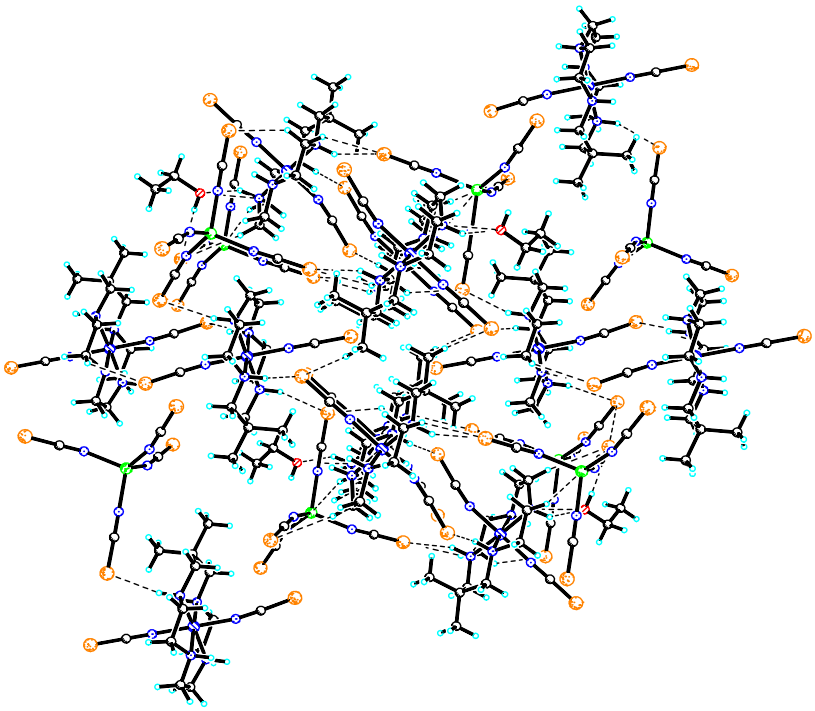

Figure 2.25: Packing diagram of COCO showing the possible intermolecular hydrogen bonding. Hydrogen atoms have been omitted for clarity.

2.13 Conclusion

The structures of nine Curtis macrocyclic compounds were solved using traditional X-ray crystallographic techniques to give accurate structural models. Comparisons of the macrocyclic structures have been made highlighting the important differences. All structures were modeled to give the best possible solution that makes chemical sense, rather than the best possible refinement value. All disorder was modeled appropriately and explained as fully as possible.

During this project knowledge about the practical aspects of crystallography was achieved such as how to choose an appropriate crystal by looking at extinction under polarized light. If a crystal has good extinction it indicates that all the molecules are aligned within the crystal and hence it is a single crystal. The reciprocal lattice was used in the determination of the unit cell by measuring the cell lengths; a, b, c, and angles; α, β, γ. Knowledge of how to locate signs of higher crystal systems in the reciprocal lattice, via systematic absences, was also gained. Structures were solved using direct

methods and when this failed the Patterson vector method was employed to locate heavy atoms. The Patterson synthesis worked well on the necessary Curtis structures because they all contained transition metal ions. The resulting electron density map was used in figuring out the structure of the molecule and then refined using least-squares refinement. Any resulting disorder was modeled so that it made the most chemical sense.

Chapter 3

3 Synthesis of Ligand 1 (L1)

3.1 Introduction to L1

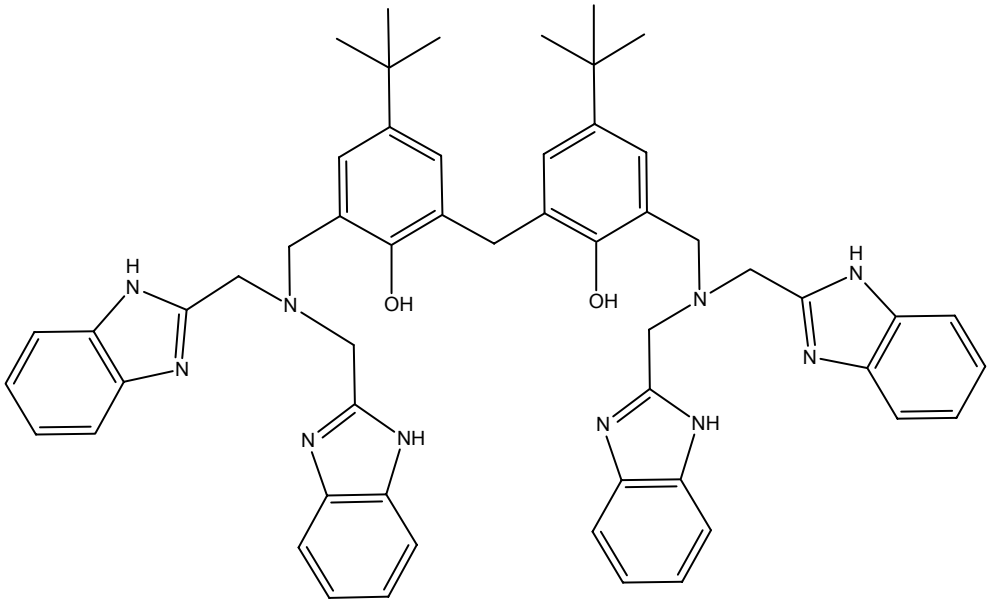

Figure 3.1: 2,2-(N,N'-bis(benzimidazole-2-ylmethyl)methylamino-5,5'-ditertiobutyl-3,3'-methanediyl-dibenzyl alcohol (L1)

The proposed ligand, L1, is composed of the head-unit DHTMBA with two BBIM pendant arms. It is a compartmental ligand with the BBIM arms acting as a "compartment" each. Thus, when it is complexed with metals, it is anticipated that at least two metal ions (M^{n+}) will coordinate with each one being in an individual BBIM arm. Because the head-unit has two phenol groups it is also possible that a third metal ion will coordinate between the two arms. This could be dependent on external factors such as pH, solvent polarity and redox state of the metal. It was anticipated that the head-unit could link at any of the nitrogen atoms shown in the BBIM ligand. However under neutral or acidic conditions the aliphatic nitrogen atom, rather than the aromatic nitrogen atoms are more basic and therefore better nucleophiles.[54]

3.1.1 Possibility of conformational changes of L1

L1 has the possibility to undergo conformational changes due to the free rotation around the arms. This will have an effect on how many metal ions will coordinate. It is expected that each metal ion will coordinate to the amine nitrogen atoms and possibly the alcohol group. With induced changes, such as a decrease in pH, the M^{n+}—O bond will break due to the increase in protons accessible to the oxygen. When the M^{n+}—O bond is broken the pendant arms will move apart to create room in the centre of the molecule (figure 3.2). Another possibility is that three metal ions will coordinate, so that the two metal ions in the arms are not bonded to the phenol groups at all. This would mean that there would be little conformational change due to the arms not being held in place by M^{n+}—O bonds.

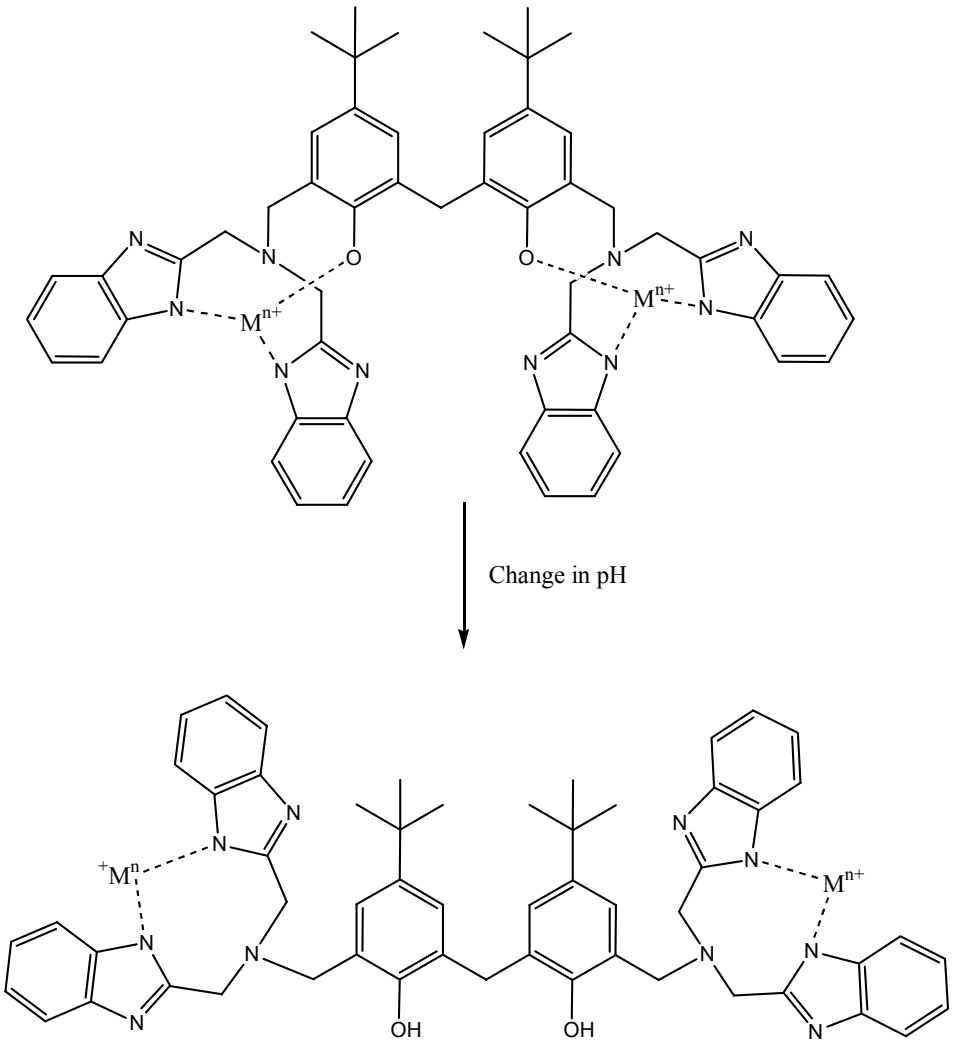

Figure 3.2: Example of possible conformational changes in L1

3.2 Results and Discussion

The intention in this project was to synthesize L1 (figure 3.3) and consequently complex it with metal ions. However there were difficulties and the synthesis of L1 was not confirmed. This chapter discusses the different attempted syntheses.

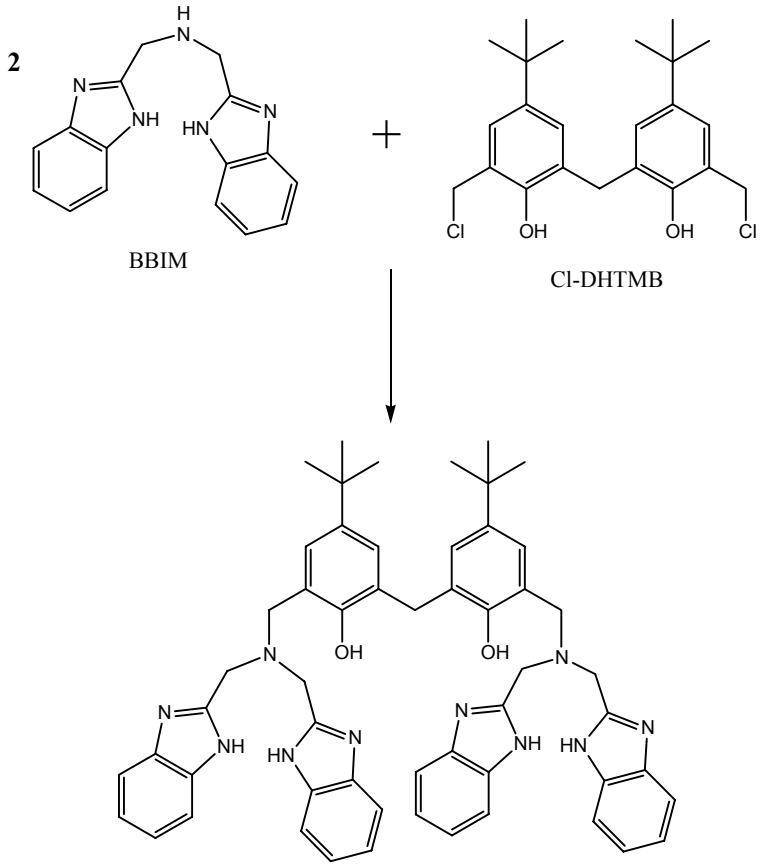

Figure 3.3: Proposed synthesis of L1.

3.2.1 BBIM

BBIM was synthesized according to Adams *et al*[55] (figure 3.4).

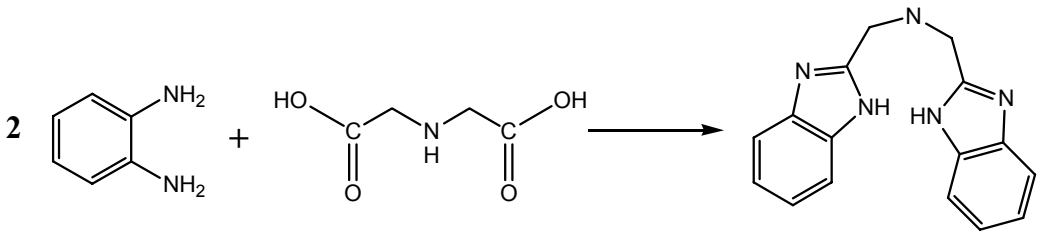

Figure 3.4: Reaction of the synthesis of BBIM.

Iminodiacetic acid was ground with two equivalents of 1,2-diaminobenzene using a mortar and pestle. This homogenous powder was heated to 200˚C over an oil bath for

two hours. On cooling this mixture turned into a black, solid, glass-like substance. This was dissolved, with quite a bit of difficulty, in hot 4 $molL^{-1}$ hydrochloric acid to give a pale blue precipitate of the trihydrochloride salt[55] that was filtered under vacuum. This precipitate was mixed with water and brought to reflux in an excess of potassium hydroxide to remove the excess hydrochloric acid. The solution turned pink. The residual precipitate was dissolved in methanol and refluxed for 20 minutes with activated charcoal. The solution was filtered under vacuum and left overnight in the fridge to give an off-white precipitate. This was recrystallized from methanol-water several times to give white needles which were characterised using X-ray crystallography, ^1H NMR and IR.

3.2.1.1 X-ray *Crystallography*

Crystals suitable for X-ray diffraction were obtained after four recrystallizations in a $MeOH/H_2O$ solution, being careful not to add too much water as the crystals are not soluble in water. This can cause the crystals to form too quickly and be unsuitable for X-ray crystallography.

It was found that BBIM crystallizes in the orthorhombic space group $Pca2_1$. The asymmetric unit consists of two BBIM molecules and eight water molecules (figure 3.5(a)). The structure was refined to 5.5%. The absolute configuration could not be determined with Mo radiation so the Friedel equivalents were merged. Anomolous scattering is higher for heavy atoms and longer wavelength radiation.[56] BBIM has no heavy atoms which is the reason the absolute configuration could not be determined. The angle between the mean plane of each benzimidazole within a molecule was 35.83˚. Therefore one benzimidazole group was rotated 35.83˚ with respect to the other benzimidazole within the molecule (figure 3.5(a)). The packing diagram (3.5(b)) illustrates how individual layers of the macrocycles are formed with water molecules in between. This diagram shows hydrogen bonding between the water molecules and the amine hydrogen atoms, however this could not be confirmed. This is most likely due to the amount of water molecules present because although the water hydrogen atoms were located in the electron density map, their positions were subsequently fixed.

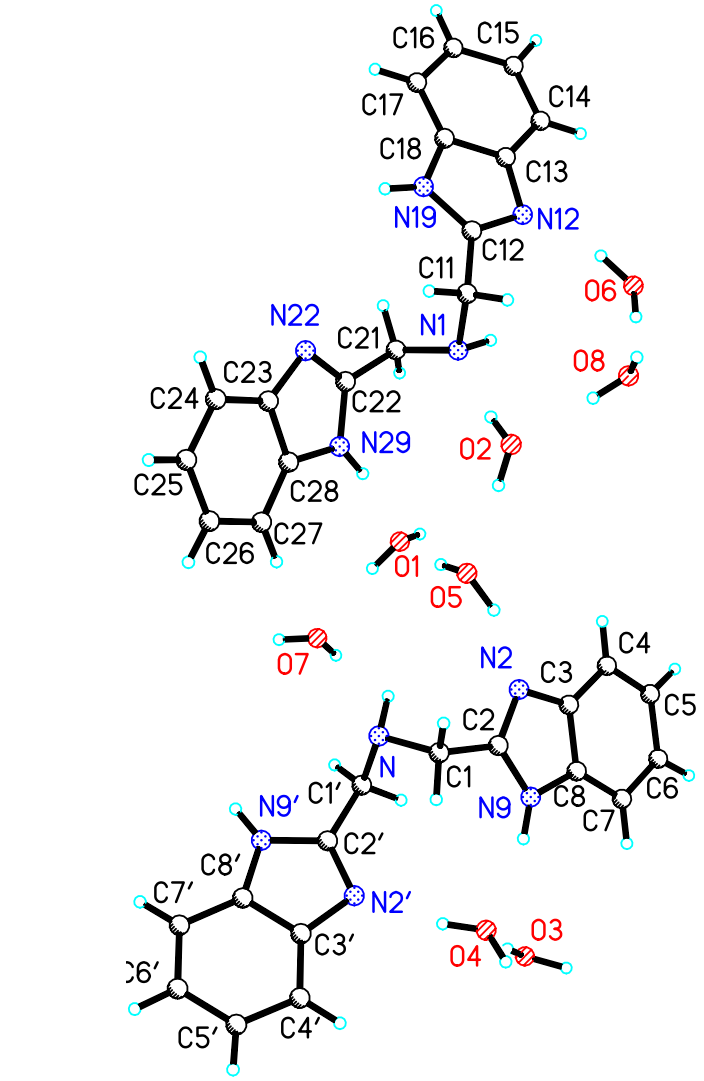

(a)

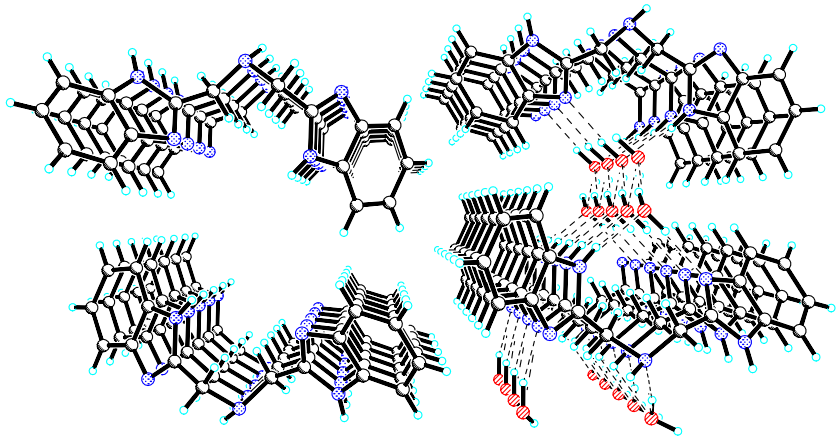

(b)

Figure 3.5: Diagram of (a) the asymmetric unit of BBIM that consists of two BBIM molecules and eight water molecules (b) packing of BBIM molecules illustrating how they line up

3.2.1.2 NMR spectroscopy

The ^{1}H NMR spectrum is virtually identical to the NMR obtained in the original synthesis.[55] It consists of a singlet at 4.1 ppm which was assigned to the four CH_2 protons on either side of the central amine. There are also two $H_{AA'BB'}$ multiplets representing four identical aryl protons each. $H_{AA'BB'}$ coupling arises from the protons being chemically equivalent but magnetically inequivalent.[57]

3.2.1.3 IR

The IR of BBIM shows a peak at 1275 cm^{-1} which is characteristic of aromatic amines.[58] This is at a higher frequency to the secondary amine, which shows a peak at 1082 cm^{-1}, because the *"force constant of the C-N bond is increased by resonance with the ring."*[58] There is a peak at 1447 cm^{-1} indicative of a 1,2-disubstituted benzene.

3.2.2 DHTMBA

The synthesis of DHTMBA caused many problems. Although DHTMBA was eventually synthesized successfully, it was in low yield (3.9%) compared with the 29% obtained in the literature.[59] It is a time consuming synthesis due to the fact that the reaction mixture has to stir for at least seven days and it could not be repeated effectively. DHTMBA was synthesized following the literature procedure[59] (figure 3.6). *Tert*-butylphenol was reacted with formaldehyde in a 1:1.5 ratio in aqueous NaOH for eight days at 50˚C. Extreme caution to avoid any O_2 contamination was taken and drying lines were added to the nitrogen. After a number of attempts it was established that that the departmental nitrogen supply was of poor quality and contained a significant amount of oxygen. The literature procedure was modified and argon, rather than nitrogen was used. After eight days the reaction mixture was cooled and the resulting resinous precipitate was filtered and washed with acetone to give a yellow solution. The solution was acidified with cold acetic acid and then extracted with ether. The ether layer was washed with water and dried over $MgSO_4$. The solvent was removed under vacuum to give an oil which was crystallized in a toluene/pet ether solution. In the crystallization attempts toluene was used instead of benzene because it is less toxic.

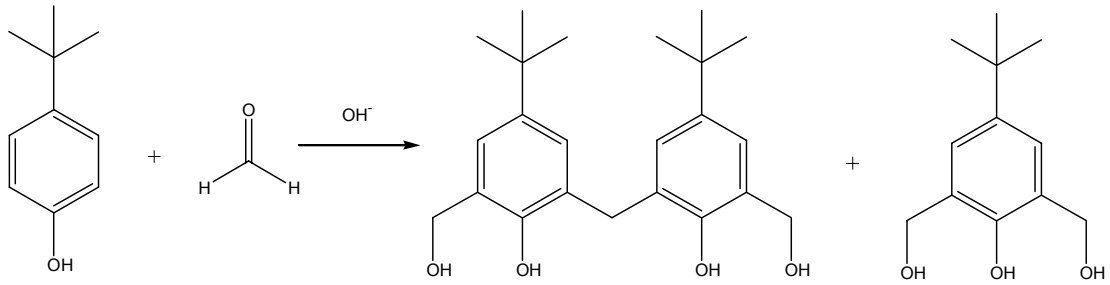

Figure 3.6: Synthesis of DHTMBA

3.2.2.1 Problems with this synthesis

The key problem with this synthesis was that the major product obtained was predominantly the single ring analogue (BTBP). In all but one synthesis where DHTMBA was isolated, the recrystallization product was BTBP. In many attempts an oil was obtained and the NMR spectrum showed a mixture of the two products with the major product being BTBP. Figure 3.7 shows proposed mechanisms for the formation of these two products. Step four appears to be the most critical. It is at this step where the reaction will proceed to form either DHTMBA or BTBP. In the formation of DHTMBA, a water molecule must be lost from the product which could be a reason this is not the favoured product, as the reaction is in aqueous solution. If the reaction does not lose water and goes on to form the one-armed single ring analogue, 2-hydroxymethyl-4-*tert*-butylphenol, it can be assumed that this is the favoured mechanism. If this is the case then it can also be assumed that this reaction will occur again to form BTBP, rather than the condensation reaction to form the dimer, DHTMBA.

The same thing can, of course, be said for the condensation reaction. If this is the preferred path then polycondesation could be a major problem, rather than the formation of BTBP.[54] This is a problem in the synthesis of DHTMBA. After the initial reaction a large amount of a gluggy precipitate is filtered, which is thought to be polymers and calixarenes. The reaction to synthesize BTBP would also be more likely to occur if there was an excess of formaldehyde. The ratio of *tert*-butylphenol to formaldehyde needs to be only 1:1.5 for the formation of DHTMBA and 1:2 for the formation of BTBP. The proportions of formaldehyde were lowered as more attempts were made to produce DHTMBA, however this appeared to have little effect. This could be due to an increase in the formation of calixarene-type molecules because

these would be more favoured as less formaldehyde is added. If more calixarenes and polymers are forming then it is also possible that the other product in the reaction would be BTBP, due to a decrease in the amount of formaldehyde being used to form the polymers.

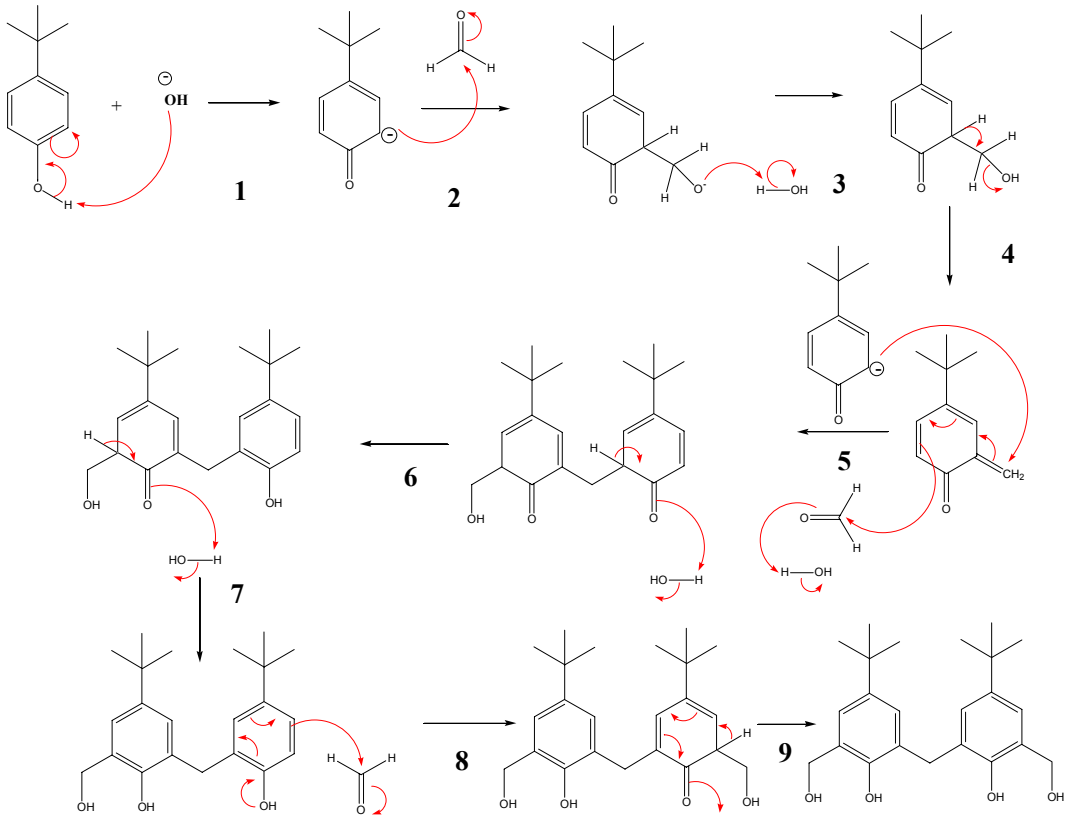

Proposed Mechanism for the formation of DHTMB

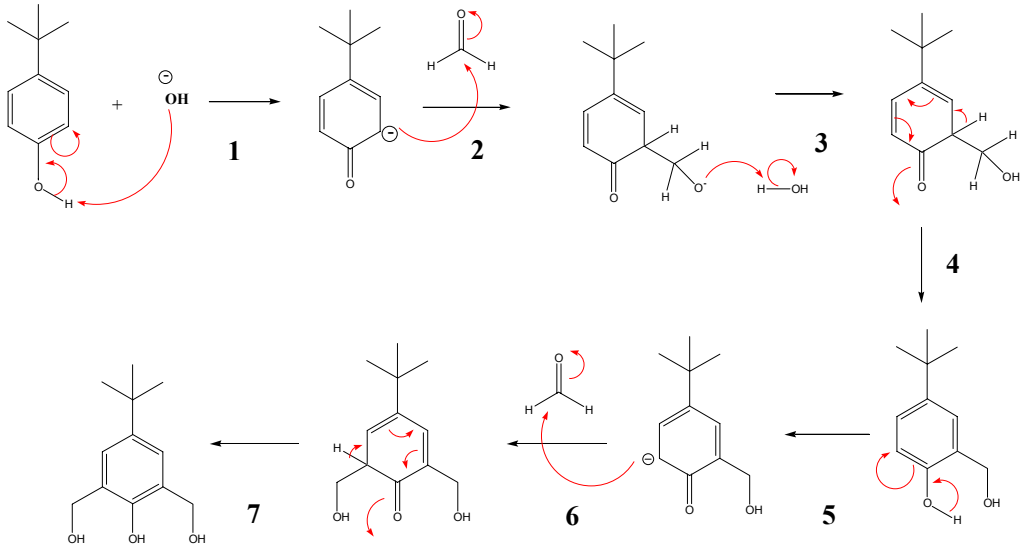

Proposed mechanism for the formation of BTBP

Figure 3.7: Proposed mechanisms for the formation of DHTMBA and BTBP respectively.

Another major problem was chemical contamination. At the beginning of the project the DHTMBA synthesis was attempted several times before it was realised that the formaldehyde being used had decomposed to give *para*-formaldeyde. This has the obvious consequence of forming polymeric molecules of different masses and hence no product was obtained. In an attempt to speed up the process to get to L1, an amount of DHTMBA was obtained from an external source. This was thought to be pure and was consequently used with no appropriate attempt to characterise it. After a number of attempts at the synthesis of Cl-DHTMB it was realised that this was a mistake and consequently all other starting materials were confirmed for purity by using techniques such as NMR and distillation. Thionyl chloride is an example. Thionyl chloride was freshly distilled before any subsequent chlorination reaction.

3.2.2.2 NMR

DHTMBA and BTBP were both characterized using ^{1}H NMR. The two spectra differ in that the DHTMBA spectrum has a singlet at 3.9 ppm representing the CH_2 group between the two aryl rings. It also has two doublets at 7.3 ppm and 6.9 ppm representing the aryl protons. It was not possible to distinguish between the two doublets. On the BTBP spectrum there is a singlet at 7.0 ppm representing the two aryl protons. The other two singlets representing the tertiary butyl and the CH_2 groups are almost indistinguishable from the DHTMBA analogues.

3.2.2.3 Mass Spectrometry

Electron Impact-Mass Spectrometry (EI-MS) emphasized the NMR results in both DHTMBA and BTBP.

BTBP *m/z* calculated = 210.1

m/z found = 210

High resolution EI-MS was run on DHTMBA to give an accurate mass of 372.23 which corresponds with the calculated mass of 372.23.

3.2.2.4 X-ray Crystallography

Crystals of BTBP suitable for crystallography were obtained by crystallization from a toluene/pet ether mixture. The structure was solved in the monoclinic space group C2/c, with a refinement value of 5.6%. The asymmetric unit consists of one BTBP molecule and two highly disordered solvate toluene molecules. The occupancy of the

toluene molecules was refined, which indicated that each atom had a quarter occupancy. Hence each atom was consequently fixed at one quarter.

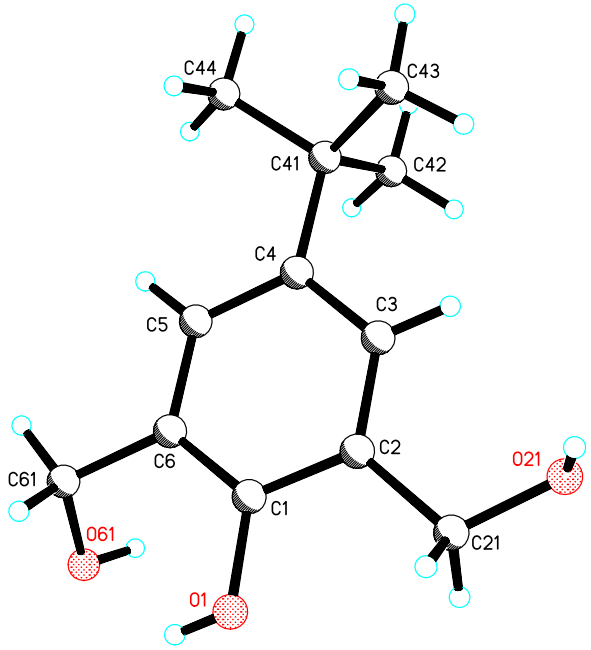

Figure 3.8: Diagram of the structure of BTBP with solvate molecules omitted for clarity.

3.2.3 DHMMBA

Due to the difficulty in synthesizing DHTMBA it was decided to attempt the synthesis of DHMMBA (figure 3.9). This was a much more ideal synthesis simply because the reaction only runs for eight hours as opposed to seven days. The synthesis was followed according to the literature.[60] An excess of formaldehyde was reacted with *p*-cresol in 30% NaOH under an argon atmosphere for three hours at 50˚C and then another five hours at 80˚C. This was then worked up and recrystallized from ethyl acetate. This still produced the single ring analogue but precipitate of DHMMBA was also obtained.

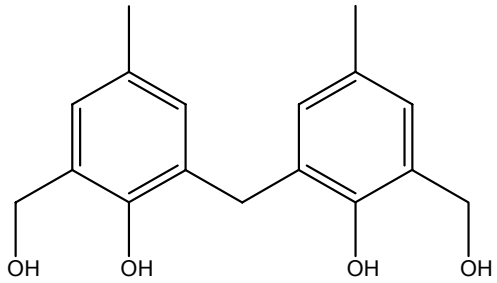

Figure 3.9: DHMMBA

This was the second synthesis of DHMMBA. Another synthesis from the literature[61] was used first. This is very similar to the synthesis described above. The key difference is that the reaction was only stirred for six hours at 60˚C before it was worked up to give the crude product which was recrystallized in ethyl acetate.

3.2.3.1 NMR

The NMR confirms the structure of DHMMBA. It is very similar to that of DHTMBA but the methyl peak at 2.2 ppm is shifted downfield compared to the *tert*-butyl peak. Also in DHMMBA there are two singlet peaks at 6.9 ppm and 6.8 ppm which represent the aryl protons.

3.2.4 Cl-DHTMB

The Cl-DHTMB synthesis was followed from the literature.[62] DHTMBA was dissolved in dichloromethane (DCM). $SOCl_2$ was dissolved in DCM and added to the DHTMBA solution over half an hour. The solution was stirred for three hours at room temperature. The solvent was removed under vacuum. The resulting yellow oil was redissolved in DCM which was removed under vacuum a further four times to ensure that all unreacted $SOCl_2$ was removed from the product. Attempts at crystallization were made by dissolving in a DCM/pet ether solution. This only ever resulted in an oil forming. It was realised later that this was most likely due to impure starting materials.

3.2.5 Cl-DHMMB

Cl-DHMMB was synthesized following the literature procedure.[63] DHMMBA was dissolved in dry benzene. $SOCl_2$ was dissolved in dry benzene and added to the DHMMBA solution over half an hour. The solution was stirred for five hours at room temperature in an argon atmosphere. The solvent was removed under vacuum and resulting solid was recrystallized in benzene to give crystals suitable for X-ray crystallography. The crystal structure of Cl-DHMMB was previously unreported. Cl-DHMMB was also characterised using ^{1}H NMR and IR.

3.2.5.1 NMR of Cl-DHMMB

^{1}H NMR of Cl-DHMMB was virtually indistinguishable from that of DHMMBA.

3.2.5.2 IR of Cl-DHMMB

The IR shows a peak at 1446 cm^{-1} which is representative of a $–CH_2$—halogen group. The phenol groups are indicated by the sharp peak at 3631 cm^{-1}. The substituted benzene rings are indicated by the peak at 1483 cm^{-1}.[58]

3.2.5.3 X-ray *crystallography of Cl-DHMMB*

Crystals suitable for X-ray diffraction were grown by recrystallization in benzene and being placed in the fridge for three days. Cl-DHMMB was found to crystallize in the triclinic space group, P-1. This was refined to 3.5%. The asymmetric unit contains one Cl-DHMMB molecule and one water solvate molecule (figure 3.10). The two phenol rings within the molecule are inclined towards each other with an angle of 113.75˚.

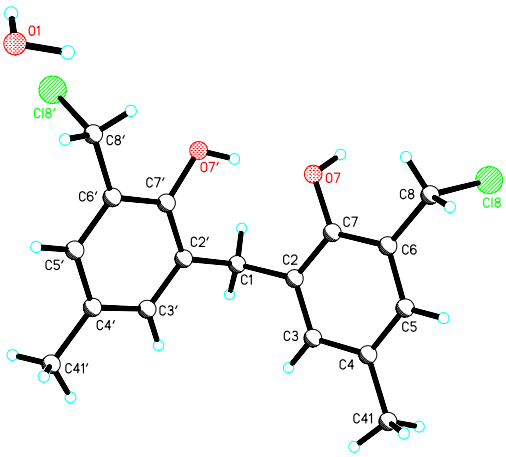

Figure 3.10: Diagram illustrating the structure of the asymmetric unit of Cl-DHMMA

Within the unit cell there are distinct layers, both horizontal and vertical, of molecules (figure 3.11). These layers are connected through hydrogen bonding between molecules which are diagonally aligned. There is an intramolecular hydrogen bond between O7'—H7' and O7 with the H7'—O7 distance being 1.81Å.

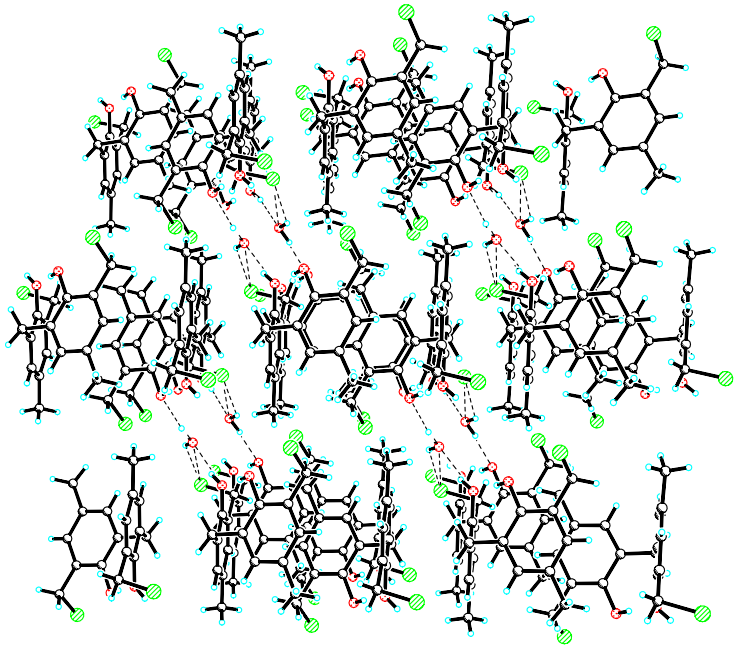

Figure 3.11: Packing diagram showing the hydrogen bonding between layers of molecules.

3.3 Ligand 1

The synthesis of ligand one was attempted a number of times following a literature procedure.[62] Due to the difficulties synthesizing DHTMBA, the methyl analogue, DHMMBA was used which resulted in L1 changing to 2,2-(N,N'-bis(benzimidazole-2-ylmethyl)methyl amine-5,5'-dimethyl-3,3'methanediyl-dibenzyl alcohol. Cl-DHMMB was reacted in a 1:2 ratio with BBIM in THF (figure 3.12). An excess of triethylamine was added to deprotonate the amine nitrogen atoms. This nucleophilic nitrogen should consequently attack the carbon attached to the chlorine atom on Cl-DHMMB, to form L1. This was not observed however. A major problem with this synthesis is that there are too many potential nucleophiles. So the triethylamine not only has the possibility of deprotonating the intended amine, but also the other nitrogen atoms on the benzimidazole and the hydroxyl groups on the head-unit.

After the reactants were stirred overnight at room temperature, a precipitate from the triethylamine salt was filtered under vacuum. The filtrate was removed under vacuum to give a white-brown solid. It was then attempted to dissolve this in HCl so that the solution could be washed with DCM to remove the excess Cl-DHMMB.[64] It was found that the solid would not redissolve at all in acid, even in concentrated HCl. Analysis of the ^{1}H NMR of this solid revealed that the product does not appear to have the BBIM ligands present. The peaks observed from BBIM in the region of 7.0-7.6 ppm were absent in the NMR of the L1 product. This means that it is most likely that the Cl-DHMMB ligands were reacting with each other to form polymers or calixarene type molecules.

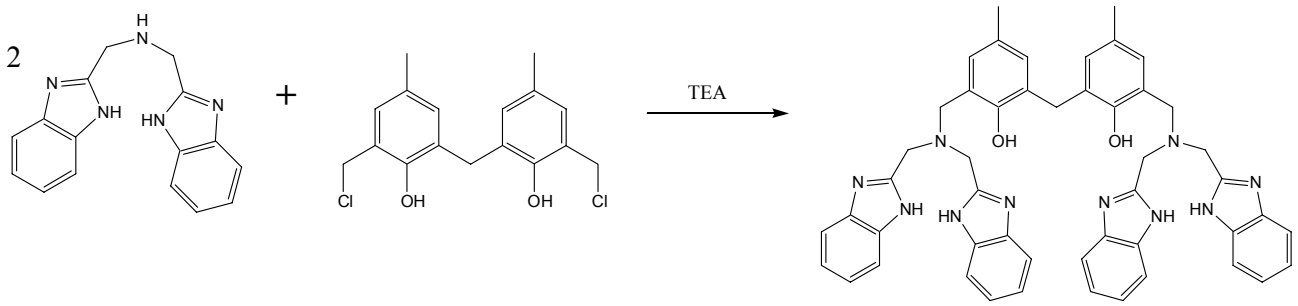

Figure 3.12: Proposed reaction for the formation of L1

3.4 Conclusion and Future Work

This chapter covered the different attempted syntheses in the bid to make L1. As previously discussed, L1 is a compartmental ligand composed of a head-unit and two pendant arms. The pendant arms, consisting of BBIM ligands, were successfully synthesized many times in preparation for the reaction with Cl-DHMMB to form L1. This was confirmed by ^{1}H NMR, IR and x-ray crystallography.

The synthesis of the head-unit DHTMBA was accomplished after many attempts and changing the reaction conditions such as; the gas to produce the inert atmosphere from nitrogen to argon, paraformaldehyde to pure formaldehyde, the ratios of formaldehyde with *tert*-butylphenol and the length of the reaction was extended slightly. Utimately it was decided that this reaction was very time consuming and quite unproductive, so it was decided to attempt another synthesis entirely. This was the synthesis of DHMMBA.

DHMMBA was successfully synthesized and characterized using ^{1}H NMR and IR and high resolution MS. This was subsequently converted to the chlorine analogue in high yield (76%). Cl-DHMMB was characterized from ^{1}H NMR, IR and x-ray crystallography.

The synthesis of L1 was attempted but proved to be unsuccessful. This is because there were too many potential nucleophiles in the reaction mixture. It appeared that the triethylamine deprotonated the hydroxyl groups on the head-unit and consequently reacted with other Cl-DHMMB units. Ideally this synthesis would be repeated with the hydroxyl groups unavailable to react. This could be achieved by protecting them via methylation. If the hydroxyl groups were methylated, the only other potential nucleophiles in the system would be the nitrogen atoms from the BBIM ligand. The proton on the nitrogen that is not part of the imidazole ring is the most acidic because the imidazole nitrogens have their electron density pulled into the л orbitals. Therefore if the hydroxyl groups are unable to react it can be assumed that the reaction would occur at the alphatic amine rather than the aromatic amine.

The synthesis of L1 also had an excess of triethylamine. This could be reduced so that there is an equivalent amount of BBIM and triethylamine so that if the reaction proceeds as planned there will not be excess triethylamine to deprotonate the imidazole amine nitrogen atoms.

The syntheses of DHTMBA and DHMMBA have the potential to be improved. It appears that in the synthesis of DHTMBA either; a lot of calixarenes were formed, BTBP was synthesized or both calixarenes and BTBP formed with very little DHTMBA. In the patent for the synthesis of DHMMBA[60] it is indicated that the reaction takes place in two steps. The first is the addition of formaldehyde to *p*-cresol to form BTBP and then the condensation reaction to form DHMMBA.[54] This is why they start the reaction temperature at 50˚C and subsequently increase it to 80˚C after three hours. During the synthesis of DHMMBA the temperature may not have been high enough to promote the formation of the dimer, so future work would include repeating this synthesis adjusting the temperature to see what works best.

The literature in this synthesis indicates that recrystallization of DHMMBA occurs in ethyl acetate. It was found in this project that BTBP is more likely to crystallize out of

ethyl acetate before DHMMBA does. Work needs to be continued to find a better solvent for crystallization so pure product can be obtained.

A last potential problem is that the argon is still not dry enough for the reaction even though it is passed through a drying tower. Therefore another thing to try would be to pass the argon through a column of Ridox after the drying tower.[54] It is hoped that with these changes the reactions will proceed more efficiently.

3.5 Experimental

3.5.1 BBIM

1,2-diaminobenzene (21.98 g, 0.2 mol) and iminodiacetic acid (13.39 g, 0.1 mol) were ground together to a homogenous powder and heated to 200˚C for 2 hours. This was left to solidify overnight. The resulting black glass-like solid was dissolved in a 4 $molL^{-1}$ hot HCl solution to give a blue precipitate. The precipitate was added to 100 mL hot H_2O and refluxed with KOH (23.54 g, 0.4 mol) for 15 minutes. MeOH and activated charcoal were added and refluxed for a further 20 minutes. The solution was filtered and left overnight to give white crystals, which were collected under vacuum.

Yield: 8.77 g, 0.03 mol, 31%

IR: 1082 cm^{-1}, 1275 cm^{-1}, 1447 cm^{-1}

^1H NMR: (CD_3OD) 7.5 (4 H, AA'BB', J = 3 Hz, aryl H), 7.2 (4 H, AA'BB', J = 3 Hz, aryl H), 4.1 (4 H, s, CH_2)

3.5.1.1 Crystal data and structure refinement for BBIM.

Empirical formula	$C_8 H_{11.50} N_{2.50} O_2$
Formula weight	174.70
Temperature	93(2) K
Wavelength	0.71073 A

Crystal system, space group	Orthorhombic, $Pca2_1$
Unit cell dimensions	a = 24.652(3) Å α = 90 ° b = 4.6630(4) Å β = 90 ° c = 30.661(4) Å γ = 90 °
Volume	3524.6(7) A^3
Z	16
Calculated density	1.317 Mg/m^3
Absorption coefficient	0.097 mm^{-1}
F(000)	1488
Crystal size	0.68 x 0.35 x 0.04 mm
Theta range for data collection	1.65 to 28.43 deg.
Limiting indices	-23<=h<=33, -5<=k<=6, -41<=l<=40
Reflections collected / unique	16215 / 4494 [R(int) = 0.0753]
Completeness to theta = 28.43	99.3 %
Absorption correction	Multi-scan
Max. and min. transmission	0.9300 and 0.4555
Refinement method	Full-matrix least-squares on F^2
Data / restraints / parameters	4494 / 3 / 451
Goodness-of-fit on F^2	1.008
Final R indices [I>2sigma(I)]	R_1 = 0.0547, wR_2 = 0.1052
R indices (all data)	R_1 = 0.0990, wR_2 = 0.1231
Absolute structure parameter	-10(10)
Largest diff. peak and hole	0.285 and -0.265 $e.A^{-3}$

3.5.2 DHTMBA

Tert-butylphenol (45.21 g, 0.3 mol) was placed with 37% formaldehyde (60 mL, 0.5 mol), and 140 mL 10% NaOH in a three-necked round bottomed flask with argon

bubbling through for half an hour. The reaction mixture was heated to 50˚C and kept under an argon atmosphere, stirring for eight days. At the end of the eight days the resinous yellow mixture was left to cool and then filtered through three filter papers. The remaining thick yellow precipitate was rinsed in acetone, leaving a small amount of white precipitate. The resulting yellow solution was condensed under vacuum to approximately 200 mL and acidified with 200 mL acetic acid. A brown oil formed in the bottom of the white solution. The mixture was extracted with ether four times. The combined ether layers were washed with H_2O to remove the excess acetic acid and dried over $MgSO_4$. The solvent was removed under vacuum to give a yellow oil. The resulting oil was dissolved in 100 mL toluene and pet ether was added until the solution went cloudy. After three days white crystals formed.

Yield : 4.39 g, 0.01 mol, 3.9%

^{1}H NMR: ($CDCl_3$) δ 7.3 (2 H, d, J = 2.5 Hz, Aryl H), 6.9 (2 H, d, J = 2.5 Hz, Aryl H), 4.7 (4 H, s, C**H$_2$**OH), 3.9 (2 H, s, ArC**H$_2$**Ar), 1.3 (18 H, s, C(C**H$_3$**)$_3$)

3.5.2.1 Crystal data and structure refinement for BTBP

As BTBP was a side product of this reaction and it crystallized more readily, a crystal structure was obtained.

Empirical formula	$C_{26}H_{36}O_6$	
Formula weight	444.55	
Temperature	178(2) K	
Wavelength	0.71073 Å	
Crystal system, space group	Monoclinic, C2/c	
Unit cell dimensions	a = 23.6110(15) Å b = 12.9805(9) Å c = 8.7140(5) Å	α = 90˚ β = 97.412(2)˚ γ = 90˚
Volume	2648.4(3) Å^3	
Z	4	

Calculated density	1.115 Mg/m^3
Absorption coefficient	0.078 mm^{-1}
F(000)	960
Crystal size	0.70 x 0.28 x 0.05 mm
Theta range for data collection	1.74 to 32.57 deg.
Limiting indices	-35<=h<=35, -19<=k<=19, -12<=l<=13
Reflections collected / unique	26445 / 4774 [R(int) = 0.0378]
Completeness to theta = 32.57	98.7 %
Absorption correction	Multi-scan
Max. and min. transmission	0.9300 and 0.8464
Refinement method	Full-matrix least-squares on F^2
Data / restraints / parameters	4774 / 0 / 178
Goodness-of-fit on F^2	1.127
Final R indices [I>2sigma(I)]	R_1 = 0.0558, wR_2 = 0.1766
R indices (all data)	R_1 = 0.0833, wR_2 = 0.2038
Largest diff. peak and hole	1.040 and -0.330 e. $Å^{-3}$

3.5.3 DHMMBA

Para-cresol (108.1 g, 1.0 mol), 37% formaldehyde (324.0 g, 4.0 mol) and 30% NaOH (133.0 g, 1.0 mol) were stirred with argon bubbling through the reaction mixture for one hour at 50˚C. After one hour the argon was changed so that it was flowing over the system. After three hours the temperature was increased to 80˚C. After a further five hours the dark yellow solution was taken off heat and cooled by adding 15% acetic acid dropwise until the solution was neutralised. The resulting white precipitate was filtered and recrystallized in ethyl acetate.

Yield: 8.19 g, 0.05 mol, 5.2%

^{1}H NMR: (CD_3OD) δ 6.9 (2 H, s, Aryl H), 6.8 (2 H, s, Aryl H), 4.9 (4 H, s, C**H$_2$**OH), 3.8 (2 H, s, ArC**H$_2$**Ar), 2.2 (6 H, s, CH_3)

3.5.4 Cl-DHMMB

$SOCl_2$ (0.5 mL, 0.7 mmol) was dissolved in 12 mL benzene and added dropwise to a solution of DHMMBA (0.4400 g, 1 mmol) in 20 mL benzene over 30 minutes, under an argon atmosphere. The resulting yellow solution was stirred at room temperature for three hours. The solvent was removed under vacuum to give a white solid. This was recrystallized in benzene to give crystals suitable for X-ray crystallography.

Yield: 0.321 g, 0.1 mmol, 76%

^{1}H NMR: ($CDCl_3$) δ 7.1 (2 H, d, J = 2.0Hz, Aryl H), 6.9 (2 H, d, J=2.0Hz, Aryl H), 4.6 (4 H, s, C**H2**—Cl), 3.9 (2 H, s, ArC**H$_2$**Ar), 2.3 (6 H, s, C**H$_3$**)

IR: 1446 cm^{-1}, 3632 cm^{-1}, 1483 cm^{-1}

3.5.4.1 Crystal data and structure refinement for Cl-DHMMB

Empirical formula	$C_{17}H_{20}Cl_2O_3$	
Formula weight	343.23	
Temperature	178(2) K	
Wavelength	0.71073 Å	
Crystal system, space group	Triclinic, P-1	
Unit cell dimensions	a = 8.9959(2) Å b = 9.0948(2) Å c = 11.1668(2) Å	α = 73.3360(10)° β = 72.6310(10)° γ = 81.7360(10)°
Volume	833.65(3) Å^3	
Z	2	
Calculated density	1.367 Mg/m^3	
Absorption coefficient	0.399 mm^{-1}	

F(000)	360
Crystal size	0.79 x 0.40 x 0.26 mm
Theta range for data collection	2.38 to 27.59 deg.
Limiting indices	-11<=h<=11, -11<=k<=11, -14<=l<=14
Reflections collected / unique	10156 / 3682 [R(int) = 0.0120]
Completeness to theta = 25.00	99.6 %
Absorption correction	Multi-scan
Max. and min. transmission	0.9300 and 0.7734
Refinement method	Full-matrix least-squares on F^2
Data / restraints / parameters	3682 / 0 / 203
Goodness-of-fit on F^2	1.030
Final R indices [I>2sigma(I)]	R_1 = 0.0340, wR_2 = 0.0945
R indices (all data)	R_1 = 0.0354, wR_2 = 0.0960
Largest diff. peak and hole	0.582 and -0.365 e.$Å^{-3}$

3.5.4.2 Hydrogen bonds for Cl-DHMMB [Å and deg.]

D-H...A	d(D-H)	d(H...A)	d(D...A)	<(DHA)
O(7)-H(7)...O(1)	0.82	1.79	2.5894(15)	164.6
O(7')-H(7')...O(7)	0.82	1.81	2.6270(13)	176.9
O(1)-H(1C)...Cl(8)	0.91	2.53	3.1790(13)	128.9
O(1)-H(1D)...O(7')#1	0.85	1.93	2.7800(16)	173.8

Symmetry transformations used to generate equivalent atoms:

#1 -x+1,-y,-z+1

Appendix

A1 X-ray Crystallographic Tables

Table A1.1 Crystal data and structure refinement for NCA

Empirical formula	$C_{15}\ H_{33}\ Cl_4\ N_5\ Ni\ O_2\ Zn$
Formula weight	565.55
Temperature	93(2) K
Wavelength	0.71073 A
Crystal system, space group	Monoclinic, P2(1)/n
Unit cell dimensions	a = 9.3111(6) Å α = 90° b = 18.4785(11) Å β = 108.6440(10)° c = 13.2900(8) Å γ = 90°
Volume	2166.6(2) $Å^3$
Z	4
Calculated density	1.734 Mg/m^3
Absorption coefficient	2.489 mm^{-1}
F(000)	1161
Crystal size	0.80 x 0.33 x 0.03 mm
Theta range for data collection	2.36 to 26.37°
Limiting indices	-10<=h<=11, -22<=k<=22, -16<=l<=15
Reflections collected / unique	17337 / 4341 [R(int) = 0.0322]
Completeness to theta = 26.37	98.1 %

Absorption correction	Multi-scan
Max. and min. transmission	0.9300 and 0.6767
Refinement method	Full-matrix least-squares on F^2
Data / restraints / parameters	4341 / 0 / 250
Goodness-of-fit on F^2	1.046
Final R indices [I>2sigma(I)]	$R_1 = 0.0354$, $wR_2 = 0.0864$
R indices (all data)	$R_1 = 0.0505$, $wR_2 = 0.0903$
Largest diff. peak and hole	0.692 and -0.873 e.$Å^{-3}$

Table A1.1.1 Hydrogen bonds for NCA [Å and deg.]

D-H…A	d(D-H)	d(H…A)	d(D…A)	<(DHA)
N(11)-H(11)…O(1)	0.93	2.27	2.885(4)	123.4
N(11)-H(11)…O(1)#1	0.93	2.22	3.101(4)	157.0
N(8)-H(8)…Cl(4)	0.93	2.75	3.661(3)	168.5
N(1)-H(1)…Cl(3)#2	0.93	2.58	3.348(3)	140.2
N(1)-H(1)…O(1)	0.93	2.39	2.934(3)	117.4

Symmetry transformations used to generate equivalent atoms:
#1 –x+1,-y+1,-z+1 #2 –x+1/2,y+1/2,-z+1/2

Table A1.2 Crystal data and structure refinement for Co13Cl

Empirical formula	$C_{11}\ H_{26}\ Cl_3\ Co\ N_4\ O_4$
Formula weight	443.64
Temperature	93(2) K
Wavelength	0.71073 Å

Crystal system, space group	Monoclinic, P2(1)/c
Unit cell dimensions	a = 11.3365(3) Å α = 90° b = 10.6726(3) Å β = 110.9360(10)° c = 15.4075(4) Å γ = 90°
Volume	1741.08(8) $Å^3$
Z	4
Calculated density	1.692 Mg/m^3
Absorption coefficient	1.469 mm^{-1}
F(000)	920
Crystal size	0.54 x 0.26 x 0.02 mm
Theta range for data collection	2.38 to 32.65°.
Limiting indices	-8<=h<=14, -16<=k<=16, -22<=l<=21
Reflections collected / unique	15305 / 5401 [R(int) = 0.0681]
Completeness to theta = 25.00	98.0 %
Absorption correction	Multi-scan
Max. and min. transmission	0.9300 and 0.3660
Refinement method	Full-matrix least-squares on F^2
Data / restraints / parameters	5401 / 0 / 210
Goodness-of-fit on F^2	1.061
Final R indices [I>2sigma(I)]	R_1 = 0.0263, wR_2 = 0.0718
R indices (all data)	R_1 = 0.0319, wR_2 = 0.0739
Largest diff. peak and hole	0.719 and -0.606 e. $Å^{-3}$

Table A1.2.1 Hydrogen bonds for Co13Cl [Å and deg.].

D-H…A	d(D-H)	d(H…A)	d(D…A)	<(DHA)
N(1)-H(1)…O(2)#1	0.93	2.30	3.0167(14)	133.4

N(5)-H(5)…O(4)#2	0.93	2.22	2.9863(14)	138.8
N(11)-H(11)…O(3)#4	0.93	2.33	3.1126(14)	141.7

Symmetry transformations used to generate equivalent atoms:

#1 –x,-y+1,-z+1 #2 x,y-1,z #4 x,-y+3/2,z-1/2

Table A1.3 Crystal data and structure refinement for NCC.

Empirical formula	C_{19} $H_{37.25}$ Cl Cu N_5 O_4 S
Formula weight	530.84
Temperature	93(2) K
Wavelength	0.71073 Å
Crystal system, space group	Orthorhombic, Cmca
Unit cell dimensions	a = 20.548(8) Å α = 90° b = 15.531(5) Å β = 90° c = 15.581(6) Å γ = 90°
Volume	4973(3) $Å^3$
Z	8
Calculated density	1.418 Mg/m^3
Absorption coefficient	1.104 mm^{-1}
F(000)	2242
Crystal size	0.30 x 0.15 x 0.02 mm
Theta range for data collection	1.98 to 26.41°
Limiting indices	-23<=h<=25, -19<=k<=19, -17<=l<=16
Reflections collected / unique	9090 / 2349 [R(int) = 0.1152]
Completeness to theta = 26.41	88.9 %
Absorption correction	Multi-scan
Max. and min. transmission	0.9300 and 0.8130
Refinement method	Full-matrix least-squares on F^2

Data / restraints / parameters	2349 / 0 / 152
Goodness-of-fit on F^2	1.037
Final R indices [I>2sigma(I)]	$R_1 = 0.0716$, $wR_2 = 0.1354$
R indices (all data)	$R_1 = 0.1385$, $wR_2 = 0.1545$
Largest diff. peak and hole	0.623 and -0.559 e. $Å^{-3}$

Table A1.3.1 Hydrogen bonds for NCC [Å and deg.]

D-H...A	d(D-H)	d(H...A)	d(D...A)	<(DHA)
N(13)-H(13)...S(30)#3	0.93	2.82	3.709(7)	160.5
N(1)-H(1)...S(30)#4	0.93	2.92	3.801(7)	158.2

Symmetry transformations used to generate equivalent atoms:

#3 -x+1,-y+3/2,z-1/2 #4 x,y-1/2,-z+3/2

Table A1.4 Crystal data and structure refinement for NCD

Empirical formula	$C_{16}\ H_{32}\ Cl_2\ Cu\ N_4\ O_8$
Formula weight	542.90
Temperature	88(2) K
Wavelength	0.71073 Å
Crystal system, space group	Orthorhombic, Pbcn
Unit cell dimensions	a = 10.29(5) Å α = 90° b = 10.93(5) Å β = 90° c = 19.10(9) Å γ = 90°
Volume	2147(18) $Å^3$
Z	4
Calculated density	1.680 Mg/m^3

Absorption coefficient	1.319 mm^{-1}
F(000)	1132
Crystal size	0.65 x 0.50 x 0.39 mm
Theta range for data collection	2.13 to 26.69°
Limiting indices	-4<=h<=12, -12<=k<=13, -17<=l<=23
Reflections collected / unique	6168 / 2134 [R(int) = 0.0603]
Completeness to theta = 25.00	96.5 %
Absorption correction	Multi-scan
Max. and min. transmission	0.6273 and 0.4811
Refinement method	Full-matrix least-squares on F^2
Data / restraints / parameters	2134 / 0 / 144
Goodness-of-fit on F^2	1.031
Final R indices [I>2sigma(I)]	R_1 = 0.0424, wR_2 = 0.0917
R indices (all data)	R_1 = 0.0712, wR_2 = 0.0998
Largest diff. peak and hole	0.522 and -0.559 e.$Å^{-3}$

Table A1.4.1 Hydrogen bonds for NCD [A and deg.]

D-H…A	d(D-H)	d(H…A)	d(D…A)	<(DHA)
N(4)-H(4A)…O(1)#2	0.93	2.46	3.179(10)	134.3
N(4)-H(4A)…O(4)#3	0.93	2.47	3.115(13)	126.5

Symmetry transformations used to generate equivalent atoms:
#1 –x,y,-z+1/2 #2 –x+1/2,y-1/2,z #3 x-1,y,z

Table A1.5 Crystal data and structure refinement for NiCu.

Empirical formula	C20 H32 Cu N8 Ni

Formula weight	506.79
Temperature	93(2) K
Wavelength	0.71073 A
Crystal system, space group	Triclinic, P-1
Unit cell dimensions	a = 8.5092(9) Å α = 104.705(2)° b = 9.6753(10) Å β = 94.856(2)° c = 15.2274(16) Å γ = 113.002(2)°
Volume	1092.1(2) $Å^3$
Z	2
Calculated density	1.541 Mg/m^3
Absorption coefficient	1.860 mm^{-1}
F(000)	530
Crystal size	0.34 x 0.16 x 0.05 mm
Theta range for data collection	2.38 to 26.38°
Limiting indices	-10<=h<=10, -10<=k<=12, -19<=l<=16
Reflections collected / unique	6442 / 4292 [R(int) = 0.0205]
Completeness to theta = 26.38	96.0 %
Absorption correction	Semi-empirical from equivalents
Refinement method	Full-matrix least-squares on F^2
Data / restraints / parameters	4292 / 0 / 282
Goodness-of-fit on F^2	1.032
Final R indices [I>2sigma(I)]	R_1 = 0.0278, wR_2 = 0.0692
R indices (all data)	R_1 = 0.0353, wR_2 = 0.0722
Largest diff. peak and hole	0.705 and -0.431 e. $Å^{-3}$

Table A1.5.1 Hydrogen bonds for NiCu [A and deg.]

D-H…A	d(D-H)	d(H…A)	d(D…A)	<(DHA)
N(8)-H(8)…N(31)	0.93	2.53	3.328(3)	144.5
N(11)-H(11)…N(33)#3	0.93	2.26	3.000(3)	136.3

Symmetry transformations used to generate equivalent atoms:

#1 –x+1,-y+1,-z+1 #2 –x+1,-y+1,-z #3 x+1,y+1,z

Table A1.6 Crystal data and structure refinement for NiMeKF

Empirical formula	C_{12} H_{28} Cl_4 N_4 Ni Zn
Formula weight	494.26
Temperature	273(2) K
Wavelength	0.71073 Å
Crystal system, space group	Tetragonal, $P4_12_12$
Unit cell dimensions	a = 11.1100(3) Å α = 90° b = 11.1100(3) Å β = 90° c = 31.9049(14) Å γ = 90°
Volume	3938.1(2) $Å^3$
Z	8
Calculated density	1.667 Mg/m^3
Absorption coefficient	2.717 mm^{-1}
F(000)	2032
Crystal size	0.60 x 0.60 x 0.30 mm
Theta range for data collection	1.94 to 32.78 °.
Limiting indices	-16<=h<=16, -16<=k<=8, -46<=l<=46
Reflections collected / unique	39499 / 6682 [R(int) = 0.0250]
Completeness to theta = 25.00	99.8 %

Absorption correction	Multi-scan
Max. and min. transmission	0.9300 and 0.6827
Refinement method	Full-matrix least-squares on F^2
Data / restraints / parameters	6682 / 0 / 202
Goodness-of-fit on F^2	1.271
Final R indices [I>2sigma(I)]	$R_1 = 0.0306$, $wR_2 = 0.0657$
R indices (all data)	$R_1 = 0.0313$, $wR_2 = 0.0659$
Absolute structure parameter	0.077(9)
Largest diff. peak and hole	0.902 and -0.421 e. $Å^{-3}$

Table A1.7 Crystal data and structure refinement for NiMeKFR

Empirical formula	$C_9 H_{22} Cl_4 N_4 Ni Zn$
Formula weight	452.19
Temperature	273(2) K
Wavelength	0.71073 Å
Crystal system, space group	Orthorhombic, $Pna2_1$
Unit cell dimensions	a = 15.3465(6) Å α = 90° b = 8.9305(4) Å β = 90° c = 12.5401(4) Å γ = 90°
Volume	1718.64(12) $Å^3$
Z	4
Calculated density	1.748 Mg/m^3
Absorption coefficient	3.104 mm^{-1}
F(000)	920
Crystal size	0.80 x 0.10 x 0.10 mm
Theta range for data collection	2.64 to 34.47°

Limiting indices	-22<=h<=22, -13<=k<=13, -17<=l<=19
Reflections collected / unique	19423 / 5559 [R(int) = 0.0249]
Completeness to theta = 25.00	100.0 %
Absorption correction	Semi-empirical from equivalents
Refinement method	Full-matrix least-squares on F^2
Data / restraints / parameters	5559 / 1 / 174
Goodness-of-fit on F^2	1.030
Final R indices [I>2sigma(I)]	R_1 = 0.0242, wR_2 = 0.0562
R indices (all data)	R_1 = 0.0270, wR_2 = 0.0571
Absolute structure parameter	-0.012(7)
Largest diff. peak and hole	0.845 and -0.321 $e.A^{-3}$

Table A1.7.1 Hydrogen bonds for NiMeKFR [A and deg.]

D-H…A	d(D-H)	d(H…A)	d(D…A)	<(DHA)
N(1)-H(1A)…Cl(5)#1	0.90	2.39	3.2513(17)	159.6
N(11)-H(11B)…Cl(4)#1	0.90	2.77	3.5090(18)	140.6
N(11)-H(11B)…Cl(5)#1	0.90	2.94	3.6613(18)	137.9
N(1)-H(1B)…Cl(4)#2	0.90	2.63	3.4574(18)	153.7
N(8)-H(8)…Cl(5)#2	0.91	2.82	3.4168(17)	123.9
N(11)-H(11A)…Cl(3)#2	0.90	2.42	3.3030(18)	167.9

Symmetry transformations used to generate equivalent atoms:
#1 x,y,z+1 #2 –x+1,-y,z+1/2

Table A1.8 Crystal data and structure refinement for NiMePh

Empirical formula	C_{29} H_{34} N_6 Ni O S_2

Formula weight	605.45
Temperature	87(2) K
Wavelength	0.71073 Å
Crystal system, space group	Monoclinic, P2(1)/n
Unit cell dimensions	a = 13.6337(19) Å α = 90° b = 11.0928(15) Å β = 94.166(3)° c = 19.625(3) Å γ = 90°
Volume	2960.1(7) A^3
Z	4
Calculated density	1.359 Mg/m^3
Absorption coefficient	0.830 mm^{-1}
F(000)	1272
Crystal size	0.75 x 0.40 x 0.10 mm
Theta range for data collection	2.08 to 25.00°
Limiting indices	-16<=h<=16, -13<=k<=13, -22<=l<=22
Reflections collected / unique	19202 / 4907 [R(int) = 0.0698]
Completeness to theta = 25.00	94.1 %
Absorption correction	Multi-scan
Max. and min. transmission	0.9300 and 0.5278
Refinement method	Full-matrix least-squares on F^2
Data / restraints / parameters	4907 / 0 / 377
Goodness-of-fit on F^2	1.068
Final R indices [I>2sigma(I)]	R_1 = 0.0721, wR_2 = 0.1626
R indices (all data)	R_1 = 0.1364, wR_2 = 0.2077
Largest diff. peak and hole	1.005 and -1.167 e. $Å^{-3}$

Table A1.8.1 Hydrogen bonds for NiMePh [Å and deg.]

D-H…A	d(D-H)	d(H…A)	d(D…A)	<(DHA)
N(1)-H(1)…O	0.93	2.45	3.332(8)	158.4
N(4)-H(4)…S(2)#3	0.93	2.58	3.477(6)	161.3
N(1')-H(1')…O#4	0.93	2.62	3.502(9)	158.2

Symmetry transformations used to generate equivalent atoms:

#1 –x,-y+1,-z #2 –x+2,-y+1,-z+1 #3 x-1/2,-y+3/2,z-1/2

#4 –x+3/2,y+1/2,-z+1/2

Table A1.9 Crystal data and structure refinement for COCO

Empirical formula	C_{16} H_{29} Co N_8 $O_{0.50}$ S_4 $Zn_{0.50}$
Formula weight	561.33
Temperature	93(2) K
Wavelength	0.71073 Å
Crystal system, space group	Triclinic, P-1
Unit cell dimensions	a = 9.9776(6) Å α = 70.511(2)° b = 14.0647(8) Å β = 82.199(2)° c = 19.5864(10) Å γ = 71.989(2)°
Volume	2462.5(2) $Å^3$
Z	4
Calculated density	1.514 Mg/m^3
Absorption coefficient	1.534 mm^{-1}
F(000)	1164
Crystal size	0.45 x 0.45 x 0.18 mm
Theta range for data collection	1.10 to 25.04°
Limiting indices	-8<=h<=11, -16<=k<=15, -23<=l<=23

Reflections collected / unique	13841 / 7155 [R(int) = 0.0136]
Completeness to theta = 25.00	82.2 %
Absorption correction	Multi-scan
Max. and min. transmission	0.9300 and 0.7211
Refinement method	Full-matrix least-squares on F^2
Data / restraints / parameters	7155 / 0 / 547
Goodness-of-fit on F^2	0.908
Final R indices [I>2sigma(I)]	R_1 = 0.0190, wR_2 = 0.0479
R indices (all data)	R_1 = 0.0208, wR_2 = 0.0492
Largest diff. peak and hole	0.273 and -0.250 e. $Å^{-3}$

Table A1.9.1 Hydrogen bonds for COCO [Å and deg.]

D-H…A	d(D-H)	d(H…A)	d(D…A)	<(DHA)
N(1)-H(1)…S(31)#1	0.93	2.53	3.3951(15)	155.5
N(1")-H(1")…O(1)#1	0.93	2.18	2.931(2)	137.8
N(4)-H(4)…S(4')	0.93	2.59	3.4016(14)	145.7
N(8)-H(8)…S(32)#2	0.93	2.68	3.4386(15)	139.6
N(11)-H(11)…S(1')#3	0.93	2.58	3.3085(15)	135.5
N(4")-H(4")…S(3')#4	0.93	2.61	3.3608(15)	138.7
N(8")-H(8")…S(33)#5	0.93	2.60	3.3332(14)	136.5

Symmetry transformations used to generate equivalent atoms:

#1 x+1,y,z #2 x,y+1,z #3 –x+1,-y+1,-z #4 –x+1,-y+2,-z+1

#5 –x+1,-y+1,-z+1

References

1. N. F. Curtis, D. A. House. *Chemistry and Industry -- London* **1961**, 1708-9.
2. Curtis, N. F., *N Macrocyclic Ligands*, **2003**.
3. Wikaira, J., *PhD Thesis*, University of Canterbury, **1996**.
4. Pilkington, R. R. N. H. *Australian Journal of Chemistry* **1970,** *23*, 2225-2236.
5. Abe, K.; Matsufuji, K.; Ohba, M.; Okawa, H. *Inorganic Chemistry* **2002,** *41*, 4461-4467.
6. Karthikeyan, S.; Rajendiran, T. M.; Kannappan, R.; Mahalakshmy, R.; Venkatesan, R.; Rao, P. S. *Proc. Indian Acad. Sci. (Chem. Sci.)* **2001,** *113*, 245-256.
7. McKee, V.; Fontecha, J. B.; Goetz, S. *Angew. Chem. Int. Ed.* **2002,** *41*, 4553-4556.
8. McKee, V.; Fontecha, J. B.; Goetz, S. *Dalton Transactions* **2005,** *5*, 923-929.
9. Nanda, K. K.; Venkatsubramanian, K.; Majumdar, D.; Nag, K. *Inorganic Chemistry* **1994,** *33*, 1581-2.
10. Constable, E. C. *Coordination Chemistry of Macrocyclic Compounds*; Oxford University Press: New York, **1999**; Vol. 72.
11. Wikipedia Foundation, I., **2006**; p. http://en.wikipedia.org/wiki/Methane_monooxygenase
12. Kaim, W.; Schwederski, B. *Bioinorganic Chemistry: Inorganic Elements in the Chemistry of Life*; John Wiley & Sons Ltd: England, **1996**.
13. Patch, M. G.; Choi, H.-k.; Chapman, D. R.; Bau, R.; McKee, V.; Reed, C. A. *Inorganic Chemistry* **1990,** *29*, 110-119.
14. Hall, D. O.; Rao, K. K. *Photosynthesis Sixth Edition*; Cambridge University Press: Cambridge, **1999**.
15. Wikaira, J.; Gorun, S. M. In *Bioinorganic Catalysis;* Reedijk, J.; Bouwman, E. Eds.; Marcel Dekker, Inc: New York, **1999**; pp. 395-408.
16. Fenton, D. E.; Gayda, S. E. *Journal of the Chemical Society, Dalton Transactions* **1977**, 2095-2101.

17. Linert, O. C. W. *Metal Mediated Template Synthesis of Ligands*; World Scientific Publishing Co. Pte. Ltd, **2004**.
18. Adams, H.; Clunas, S.; Cummings, L. R.; Fenton, D. E.; McHugh, P. E. *Inorganic Chemistry Communications* **2003,** *6*, 837-840.
19. Adams, H.; Clunas, S.; Fenton, D. E. *Acta Crystallographica Section E* **2004,** *60*, 338-339.
20. Adams, H.; Clunas, S.; Fenton, D. E.; Gregson, T. J.; McHugh, P. E.; Spey, S. E. *Inorganica Chimica Acta* **2003,** *346*, 239-247.
21. Flomer, W. A.; O'Neal, S. C.; Kolis, J. W.; Jeter, D.; Cordes, A. W. *Inorganic Chemistry* **1988,** *27*, 971-973.
22. Fontecha, J. B.; McKee, V. *Personal Communication*, **2005**.
23. Abuskhuna, S.; Briody, J.; McCann, M.; Devereux, M.; Kavanagh, K.; Fontecha, J. B.; McKee, V. *Polyhedron* **2004,** *23*, 1249-1255.
24. Eshwika, A.; Coyle, B.; Devereux, M.; McCann, M.; Kavanagh, K. *Biometals* **2004,** *17*, 415-422.
25. Karlin, K. D.; Zuberbuhler, A. D. In *Bioinorganic Catalysis;* Reedijk, J.; Bouwman, E. Eds.; Mark Dekker, Inc: New York, **1999**; pp. 469-534.
26. Wikipedia Foundation, I., **2006**; p. http://en.wikipedia.org/wiki/Hemocyanin.
27. Hazes, B.; Magnus, K. A.; Bonaventura, C.; Bonaventura, J.; Dauter, Z.; Kalk, K. H.; Hol, W. G. J. *Protein Science* **1993,** *2*, 597-619.
28. Volbeda, A.; Hol, W. G. J. *Journal of Molecular Biology* **1989,** *209*, 249-79.
29. McKee, V.; Zvagulis, M.; Dagdigian, J. V.; Patch, M. G.; Reed, C. A. *Journal of the American Chemical Society* **1984,** *106*, 4765-47772.
30. Gaykema, W. P. J.; Volbeda, A.; Hol, W. G. J. *Journal of Molecular Biology* **1986,** *187*, 255-275.
31. Pessiki, P. J.; Khangulov, S. V.; Ho, D. M.; Dismukes, G. C. *Journal of the American Chemical Society* **1994,** *116*, 891-897.
32. Wikaira, J.; Gorun, S. M. In *Bioinorganic Catalysis;* Reedijk, J.; Bouwman, E. Eds.; Mark Dekker, Inc: New York, **1999**; pp. 355-422.
33. Menze, M. A.; Hellmann, N.; Decker, H.; Grieshaber, M. K. *Biochemistry* **2005,** *44*, 10328-10338.
34. Perbandt, M.; Guthohrlein, E. W.; Rypniewski, W.; Idakieva, K.; Stoeva, S.; Voelter, W.; Genov, N.; Betzel, C. *Biochemistry* **2003,** *42*, 6341-6346.

35. Takano, Y.; Kubo, S.; Onishi, T.; Isobe, H.; Yoshioka, Y.; Yamaguchi, K. *Chemical Physics Letters* **2001,** *335*, 395-403.
36. Tzou, J. R.; Lou, Y. M.; Wang, S. M.; Li, N. C. *Journal of Inorganic Biochemistry* **1991,** *43*, 723-9.
37. Oberhausen, K. J. *PhD Thesis*, University of Louisville, **1990**.
38. Dolashka-Angelova, P.; Dolashki, A.; Savvides, S. N.; Hristova, R.; Van Beeumen, J.; Voelter, W.; Devreese, B.; Weser, U.; Di Muro, P.; Salvato, B.; Stevanovic, S. *Journal of Biochemistry (Tokyo, Japan)* **2005,** *138*, 303-312.
39. Spinozzi, F.; Gatto, S.; De Filippis, V.; Carsughi, F.; Di Muro, P.; Beltramini, M. *Archives of Biochemistry and Biophysics* **2005,** *439*, 42-52.
40. Dolashka-Angelova, P.; Dolashki, A.; Stevanovic, S.; Hristova, R.; Atanasov, B.; Nikolov, P.; Voelter, W. *Spectrochimica Acta, Part A: Molecular and Biomolecular Spectroscopy* **2005,** *61A*, 1207-1217.
41. Colangelo, N.; Hellmann, N.; Giomi, F.; Bubacco, L.; Di Muro, P.; Salvato, B.; Decker, H.; Beltramini, M. *Micron* **2004,** *35*, 53-54.
42. Curtis, N. F.; House, D. A. *Chem. and Ind. -- London* **1961**, 1708-9.
43. House, D. *Personal Communication* **2006**.
44. Curtis, N. F. *Coordination Chemistry Reviews* **1968,** *3*, 3-47.
45. Curtis, N. F. *Coordination Chemistry Reviews* **1968,** *3*, 4.
46. Sheldrick, G. M.: Germany, 1996.
47. Curtis, N. F.; Flood, K.; Robinson, W. T. *Polyhedron* **2006,** *25*, 1579-1584.
48. Tomkiewicz, A.; Mrozinski, J.; Bruedgam, I.; Hartl, H. *European Journal of Inorganic Chemistry* **2005**, 1787-1793.
49. Curtis, N. F. *Coordination Chemistry Reviews* **1968,** *3*, 23.
50. Curtis, N. F.; Flood, K.; Robinson, W. T. *Polyhedron* **2006,** *25*, 1601-1606.
51. Curtis, N. F.; Flood, K.; Robinson, W. T. *Polyhedron* **2006,** *25*, 1313-1318.
52. Curtis, N. F., *Personal Communication* **2005**.
53. Curtis, N. F. *N Macrocyclic Ligands*; Elsevier Ltd, **2003**.
54. Turnbull, M., *Personal Communication* **2006**.
55. Adams, H.; Bailey, N. A.; Crane, J. D.; Fenton, D. E. *Journal of the Chemical Society Dalton Transactions*. **1990**, 1727-1735.
56. Polson, M., *Personal Communication* **2006**.
57. Kemp, W. *Organic Specroscopy*, 3rd ed.; Macmillan: Edinburgh, 1992.

58. Silverstein, R. M.; Bassler, G. C.; C.Morrill, T. *Spectrometric Identification of Organic Compounds*, 4th ed.; John Wiley and Sons: Singapore, 1981.

59. Dhawan, B.; Gutsche, C. D. *Journal of Organic Chemistry* **1982,** *48*, 1536-1539.

60. (Kishimoto, Akira, Japan). Application: JP JP, 1982; p. 6

61. Haino, T.; Matsumura, K.; Harano, T.; Yamada, K.; Saijyo, Y.; Fukazawa, Y. *Tetrahedron* **1998,** *54*, 12185-12196.

62. Lambert, E.; Chabut, B.; Chardon-Noblat, S.; Deronzier, A.; Chottard, G.; Bousseksou, A.; Tuchagues, J.-P.; Laugier, J.; Bardet, M.; Latour, J.-M. *Journal of the American Chemical Society* **1997,** *119*, 9424-9437.

63. Ito, K.; Ohta, T.; Ohba, Y.; Sone, T. *Journal of Heterocyclic Chemistry* **2000,** *37*, 79-85.

64. McKee, V. *Personal Communication* **2005**.